Doctoral Dissertation

Manoeuvring and Guidance of Catamaran Wave Adaptive Modular Vessel

（Wave-Adaptive 型双胴船の操縦性能とその制御）

Pandey Jyotsna

June 2017

Graduate School of Engineering,

Osaka University

The Dissertation Committee for Pandey Jyotsna Certifies that this is the approved version of the following dissertation:

Manoeuvring and Guidance Catamaran Wave Adaptive Modular Vessel

（Wave-Adaptive 型双胴船の操縦性能とその制御）

Committee:

Associate Professor Atsuo MAKI

Professor Naoya UMEDA

Professor Yasuyuki TODA

Abstract

Autonomous path planning of the ship is a very challenging problem in terms of navigation, controller design and guidance algorithm. Specially, controller design for high speed autonomous vehicles such as Wave Adaptive Modular Vessel (WAM-V) is challenging due to uncertainty in dynamic models, significant sea disturbances, underactuated dynamics and unknown hydrodynamic parameters. Usually, highly expert and intelligent controller is required to make a suitable decision considering various environmental conditions. Hence, this thesis deals with the development of an underactuated controller for WAM-V, which is able to navigate between waypoints.

A WAM-V is a shallow-draft high speed catamaran vessel, with tremendous controllability and maneuverability. In order to fully understand the dynamic behaviour of WAM-V, MMG type of mathematical model are used. The manoeuvring behaviour of the vessel is also studied with the help of the experiments. This study is divided into two parts.

The first part of the study deals with the development of a dynamic mathematical model of WAM-V. In order to develop an accurate mathematical model, captive model tests and free running experiments are carried out. Here, MMG type of model is applied. The resistance force on a mono hull and twin hull has been investigated by captive model tests. The drift tests are also conducted in order to determine the manoeuvring derivatives. In order to study the manoeuvring characteristics of the WAM-V, speed tests and turning tests are conducted at Osaka University free running pond facility. By using system identification method, the free running experimental data are further used

to identify the unknown manoeuvring derivatives, which cannot be determined from the captive model tests.

In the second part, a fuzzy reasoned double loop controller is proposed for navigation path planning of WAM-V. In the outer loop of the controller, fuzzy controller is utilized to feed the desired heading. In the inner loop, a PID feedback controller is used to correct the desired course generated by the fuzzy reasoned algorithm. The control system provides the required feedback signals to track the desired heading obtained from the fuzzy algorithm. After PID generates the appropriate command, thrusts are allocated to the port side and starboard side thrusters. Finally, thrusts are allocated to both the thrusters based on the lookup table which is obtained from the free running model experiments. Using the proposed controller, several experiments are conducted at Osaka University free running pond facility. The proposed control scheme is successfully performed the navigation path planning.

The main conclusions obtained in this thesis are:

1. The MMG type maneuvering mathematical model has been found applicable to the model with shallow-draft and twin hull- twin propeller system such as WAM-V.

2. In order to better quantify the WAM-V dynamics with respect to autonomous control design, captive model tests and free running model test have enabled significant contribution.

3. The waypoint navigation experimental results show that the fuzzy guided waypoint controller scheme is simple, intelligent and robust.

4. The goal of this research is to present a solution to the waypoint control problem for the underactuated catamaran vessel (WAM-V), which is achieved successfully.

Acknowledgement

Foremost, I would like to express my sincere gratitude and thanks to my advisor Prof. Kazuhiko Hasegawa for accepting me as a graduate student in the Department of Naval Architecture and Ocean Engineering, Osaka University. I am also grateful to him for his continuous support of my PhD study and related research, for his patience, motivation, enthusiasm and immense knowledge. I have been trained to become a true researcher from identifying research and writing research proposals, to executing research ideas, organizing experiments, carrying out simulation, to writing concise papers and time management during my doctoral candidate's life. Without his guidance and support, this dissertation would not have been completed.

Beside my advisor, I would like to thank the rest of my thesis committee: Prof. Naoya Umeda, Prof. Yasuyuki Toda and Associate Prof. Atsuo Maki, for their encouragement, insightful comments, and hard questions.

My sincere thanks also go to Associate Prof. Atsuo Maki for becoming my official guide after the retirement of Prof. Kazuhiko Hasegawa. I am thankful for his guidance and support in writing my thesis as well as in official procedures.

I am also grateful to Researcher Hidenari Makino for his guidance and help in conducting the pond experiments. He always provided very insightful advice and comments.

I received help during the experiment and analysis from many students of Hasegawa and Umeda laboratory. I am grateful for their help.

I acknowledge the Japan Ministry of higher Education, Culture, Sports, Science and Technology (MEXT) for providing me with the opportunity to pursue graduate studies in Japan and for the generous financial support throughout my study.

There are several others whom I would like to thank collectively for the sleepless nights we were working together before deadlines, and for all the fun we have had in the last three and half years. To those who feel missed out in this listing I owe my sincere apologies.

Finally, and most importantly, I am indebted to the love and support that I have received from my family members. In special, I am thankful to my parents who made several sacrifices to ensure that I could pursue my dream of furthering the education abroad to PhD. Deepest gratitude is given to my mother for her immense emotional support and constant encouragement.

NOMENCLATURE

$C(\vec{v})$	Centripetal and Coriolis acceleration
C_t	Resistance Coefficient
CDH	Reference degree
COG	Course Over Ground
$D(\overrightarrow{v})$	Hydrodynamic Damping
$DCPA$	Distance of the closest point of approach
$DCPA'$	Non-dimensionalised value of DCPA
d_{yp} & d_{np}	Propeller Influence factor to the Y and N directions
F_n	Froude Number
$G(\overrightarrow{\eta})$	Restoring force and Moment
I_Z	Mass moment of Inertia
J_Z	Added mass moment of Inertia
L	Length of WAM-V
M	Inertia matrix
m_x	Added mass in surge direction
m_y	Added mass in sway direction
M	Vehicle's Mass
$n_{(P)}$	Revolution speed of port side propeller
$n_{(S)}$	Revolution speed of starboard side propeller
u	Surge Velocity of Vessel
v	Sway Velocity of Vessel
U	Speed of the Vessel
r	Yaw rate
S	Wetted Surface Area or Ship
$TCPA$	Time to the closest point of approach
$TCPA'$	Non-dimensionalised value of TCPA
t_p	Thrust Deduction Factor
$X_u(U)$	Total Ship Resistance
X_H, Y_H, N_H	Hydrodynamic forces and moments acting on the ship hull
X_P, Y_P, N_P	Hydrodynamic forces and moments due to propeller
x_g	Distance from CG

X_0Y_0	Earth Fixed Coordinate System
XY	Body fixed coordinate system
y_P	Distance between the propellers action points and the baseline
α	Bearing angle of the waypoint from the vessel
β	Drift angle
$\phi_{(P)}$& $\phi_{(S)}$	Turning angle of the propeller rotation
ρ	Density of water
θ	Encountering angle of waypoint from the vertical axis
Ψ	Vessel Heading
ψ_1	Order of Course
ψ_2	Shortest path to the second next Waypoint

TABLE OF CONTENTS

LIST OF FIGURES

LIST OF TABLES

1. INTRODUCTION

Science may be described as the art of systematic oversimplification.

– Karl Popper

1.1 BACKGROUND AND OBJECTIVE

The negative impact of global climate change on the ocean environment cannot be overlooked anymore, a deep insight into the ocean environment and its environmental dynamics are needed to understand the ocean environmental behaviour and its effect on the society. According to research only 5% ocean, is known, and it is one of the most demanding environments and a vast frontier for discovery. Recent studies indicated that global warming and ocean acidification have worsened, and the frequency of the adverse impacts of climate changes has increased in recent years. Additionally, an increase of human activity in the ocean and exploitation of the ocean resources has led to changes in the marine ecosystem and reduced fishery resources. Hence, in order to understand human intervention and its effect on the ocean environment, we need to nurture the next generation techniques. Currently, oceanography or ocean environmental sensing (meteorological survey) is carried out using satellites, buoys, research vessels or ships. However, remote surveillance of oceanography data using satellites is restricted due to cloud cover, temporal/geographical coverage as well as spatial resolution. Meanwhile, manned research vessels are expensive for ocean surveillance, and in situ measurement of oceanographic data. Whereas the use of moored buoy, due to lack of controllability and self- deployability is not so attractive option for spatial sampling purposes. Due to all of

the above mentioned reasons autonomous surface vehicles (ASV) & autonomous underwater vehicles (AUV), due to their various capabilities for payload, communication, and autonomy, have emerged as the best option for in situ measurement of oceanography data as well as a complimentary observing system (port protection, mine countermeasures, and surveillance missions). It is foreseen that there will be a future market for unmanned or autonomous marine vehicles capable of doing different marine operations without the assistance of a human pilot.

In 2009 Marine Advanced Research Inc. developed a new generation surface vessel called Wave Adaptive Modular Vessel (WAM-V). WAM-V technology contains a huge amount of potential in various marine applications. An autonomously navigated WAM-V can conveniently replace different dangerous coastal tasks and provide disaster assistance. Control design for WAM-V is challenging due to uncertainty in dynamic models, sea disturbances, underactuated dynamics and unknown manoevring derivatives. The purpose of this thesis is to present a solution to the waypoint navigation problem for a class of underactuated catamaran vessels. To design a robust controller, the dynamics of the system and its manoeuvring performance should be known. Simulation and experimental based study to know the system dynamics is the best solution.

Autonomous ship navigation can be divided into two major areas of research collision avoidance and path following. Path following is a very challenging problem in terms of navigation, controller design and guidance algorithm. Path tracking uses positional information, typically obtained from Global Positioning System (GPS), Inertial Measurement Unit (IMU) and vehicle odometry, to control the vessel speed and steering to follow a specified path. Ship Auto-Navigation Fuzzy Expert System (SAFES) was developed by Hasegawa et al. (1986, 1990, and 1993) for harbor

manoeuvring, congested waterway navigation and collision avoidance. This navigation path planning algorithm utilizes fuzzy theory, which is quite similar to the human control. The fuzzy control rules are constructed based on the human operator's experience. There are several guidance algorithms such as pure pursuit (PP), line of sight (LOS) and constant bearing (CB) are widely discussed in the literature for waypoint navigation and control applications (Fossen 1994). A wide range of ship collision avoidance control algorithm is based on the Convention on the International Regulations for Preventing Collisions at Sea (COLREGS), by the International Maritime Organization (IMO, 1972). A fuzzy based algorithm for collision avoiding autonomous navigation of marine vehicle was proposed under COLREGS guideline. This algorithm has the ability to handle static and/or moving obstacles (Lee et al. 2004). Beard and Maclain (2012) introduced the algorithm based on Dubins paths. It was found that the Dubin's path is an optimal (shortest) path between two waypoints. These are constructed from two circular arcs and a straight line.

Ship accidents, collision and grounding are reported during bad manoeuvring of the vessel (Zaojian, et al 2006). Understanding manoeuvring is nothing but an interplay of forces. It is an important ability of the ship to perform navigation and guidance related tasks because it is directly related to ship safety. It is composed of speed change, turning, course keeping, course change and stopping ability, etc. (Hirano & Takashima 2010). CFD based study was conducted and validated through EFD data to study the WAM-V dynamics in Calm water and Wave (Mousaviraad et a. 2013). Manoeuvring performance of a vessel is judged based on manoeuvring criteria which are briefly discussed in Chapter 4.

The dynamic behaviour of a ship can be predicted from a mathematical model,

which describes the relationship between the forces and control parameters. To analyze the manoeuvring performance of a ship and design an autopilot, we must develop a mathematical model that can precisely describe the ship's dynamic behaviour. In order to model a realistic physical mathematical model of the ship, the parameters usually known as manoeuvring derivatives should be accurate enough. Manoeuvring derivatives are obtained by various methods such as the captive model test, slender body theory, empirical formulae, computational fluid dynamics (CFD), system identification (SI), etc. Among them, the planar motion mechanism (PMM) test, a type of the captive model test, is widely used because most coefficients can be obtained (Ankudinov et al. 1993 & Abkowitz 1964).

From the foregoing and other relevant literature, it is clear that this topic is very interesting and extremely important area of study. Since WAM-V is a new generation vessel so there is a lot of potential and challenges in this study.

1.2 HISTORY OF CATAMARAN SURFACE VESSELS

The sea and its mastery were one of the greatest contributions to human civilization. The concept of multi hulls shaped boats were probably invented in the ancient era of the 16th century near south west coach of India and the English adventurer William Dampier was the first person to describe this kind of vessel in English in that era. The word Catamaran is coined from the Tamil word Kattumaram (Kattu: to tie & maram: wood tree) which means "tied wood". The craft of this design almost developed because the only available material was a hollowed out tree trunk in order to transport things from one shore to the other and necessity would have a improved large space with good stability (Lawless, et al. 2007). Early catamarans were up to 22m long and

were driven by peddling because of lack of propulsion systems and automation. The capability of catamarans was more or less ignored in the early 80's one of the reasons may be the design remains unknown in the west region of the world. The catamaran entered into the western world in 1936 when Eric de Bisschop built Kaimiloa in Hawaii. In 1870's U.S designer of America's Cup boat Nathanael Herreshoft started to use catamaran for racing and that sailed so successfully against mono hull design so sailing authorities barred them from competition for a long time and they remained barred till 1960's, but till then people recognized at this early stage that the catamaran layout offered a high speed with a large deck area (Casson, 1964). After 1960's modern history of catamaran started with the small catamarans raced successfully against the mono hull and international competition began in 1961 between the United States and Great Britain. In 1975, the first high-speed (32.19 kph) catamaran was built-in Australia for transporting tourist. The first aluminum passenger catamaran ferry was also built-in Australia and demonstrated by a company, International Catamaran (Incat) (Nordtvedt, 1996).

In the 90's as technologies have grown and the complexities of the structural design have become understood well, the size of the catamaran has grown in order to carry trucks and coaches at the high speed. Currently T-AGOS are the largest catamaran ships used by the United States Navy for ocean surveillance. Catamaran is also demonstrated having autonomous marine navigation using wind-powered propulsion (Elkaim et al. 2006). In the 20^{th} century, it was anticipated that the catamarans are established with the design and autonomously controlled. In this era, so many autonomously catamarans were successfully made the description of some of them is as follows. Figure 1.1 shows the famous catamaran boats developed in recent years.

Figure 1.1 Catamaran shape of ASV's

In 1997 MIT developed the catamarans ACES (Autonomous Coastal Exploration System) with better cruising speed; longer mission endurance and better seakeeping capabilities (Manley 1997). Autonomous catamaran Delfim was developed for the purpose of automatic marine data acquisition and as a communication relay for companion AUV in Lisbon in the year 2000 (Alves et al. 2006). Autonomous catamaran Charlie was developed for the collection of the sea surface microlayer and then upgraded for robotic research by CNR-ISSIA Genova (Caccia et al. 2008). Autonomous catamaran ROAZ was developed to support AUV missions and multiple operations with ISEP-Institute of Engineering of Porto in Portugal 2006 (Ferreira et al 2006). Autonomous catamaran Springer was developed to track and monitor water pollutants and geographical survey by University of Plymouth, U.K (Xu et al. 2006).

Multi-hulled ships have several distinct advantages over mono hull. These advantages include a larger available deck area, excellent transverse stability, and lower power consumption for a given speed (Peterson 2013).

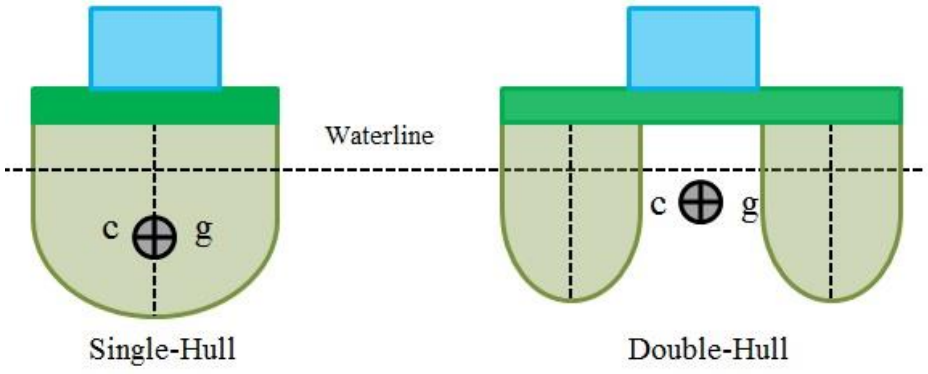

Figure 1.2 Pictorial representation of mono hull and double hull ship

Nowadays, several robotic competitions are organized in order to foster the exchange of ideas. In 2013 the Office of Naval Research (ONR) has established the Maritime RobotX Challenge. Maritime RobotX challenge is an ideal benchmark for the development of autonomous surface vessel WAM-V (AUVSI Foundation). These types of competition give an enormous contribution to the next generation technologies. This competition brings together multiple research groups working in the similar research area in different countries by providing the common task to be solved at a specific place and a specific time which fosters the exchange of ideas. The goal of the competition is to establish the vessel selecting the sensors, propulsion systems and control algorithms in order to accomplish mission tasks fully into their autonomy schema.

1.3 MAIN CONTRIBUTIONS OF THE THESIS

The contribution of this thesis is focused on a waypoint guidance and control problem for autonomous surface vessels. The thesis includes the study of manoeuvring behaviour of catamaran WAM-V vessel and also developing a mathematical model to simulate the dynamic behaviour. This thesis includes designs for solving these

objectives with analysis of the achieved performance. The results have been published in several international publications. The main contributions are listed as,

- Development of WAM-V system with its navigational and manoeuvring performance for free running and navigational experiments.
- Deriving MMG type of mathematical model for twin-hull and twin-propeller new generation WAM-V.
- Conducting the captive model test for catamaran WAM-V to study the hull resistance force and hydrodynamic force acts during motion.
- With the help of Captive model tests, free running tests and system identification method, the manoeuvring derivatives are calculated for WAM-V.
- A fuzzy guided waypoint controller implemented and successfully tested with WAM-V.
- A lookup table based thrust allocation technique is used to allocate the desired thrust able to navigate between the desired waypoints.
- The experimental outcomes of the intelligent controller are promising which is designed for guidance and navigation for WAM-V.

1.4 OUTLINE OF THE THESIS

Chapter 1, deals with the general overview of the problems regarding the development of ASV, followed by a brief review of the different and most popular ASV developed around the world for various marine applications.

In Chapter 2, the design and development of WAM-V are described. Hardware and software module in order to conduct the free running and autonomous navigation

experiments are also discussed. The various hardware modules required to develop the full system such as actuators, sensors, on-board computers, power supply and communication module are discussed in detail.

Chapter 3, deals with the development of MMG type of mathematical model to study the dynamic behaviour of WAM-V.

Chapter 4, deals with the study of manoeuvring behaviour of WAM-V in calm water. In order to study the resistance forces on a mono hull and double hull resistance tests were conducted at Osaka University Towing Tank Facility. Drift tests are also conducted in order to calculate the manoeuvring derivatives of mathematical model briefly discussed in Chapter 3. Free running tests at the Osaka University Pond Facility are also conducted in order to study the manoeuvring behaviour of WAM-V in calm water.

In chapter 5, system identification method to obtain the manoeuvring derivatives, which couldn't be calculated with the help of captive model tests is described. Finally, the maneuvering derivatives calculated with the help of captive model tests, free running tests and system identification method are presented.

In chapter 6, the waypoint guidance algorithm using fuzzy theory is discussed step by step. The fuzzy reasoning with membership function is described. The simulation study in order to study the effectiveness of the proposed waypoint guidance algorithm and controller parameter tuning, using the mathematical model described in chapter 3 are also presented.

In chapter 7, the double loop feedback controller for waypoint navigation is discussed in detail using the control system layout.

In chapter 8, the thrust allocation problem for underactuated WAM-V is discussed. A lookup table based thrust allocation methodology is described.

In chapter 9, This chapter delineates the results of the various experiment conducted to validate the effectiveness and robustness of the proposed double loop fuzzy guided waypoint controller.

In chapter 10, the conclusion of this research is presented, followed by the future work.

2. DESIGN AND CONFIGURATION OF WAM

2.1 DESIGN

A WAM-V is a shallow-draft high speed catamaran vessel, with tremendous controllability and manoeuverability. The agumentation of WAM-V with springs, shock absorbers, and ball joints, gives enough agility to the vessel and helps in damping stresses to the structure and payload. WAM-V is equipped with two propellers attached to the aft part of each pontoon with special hinges, which keep the propeller in the water all the times. Because of the shock absorbers and ball joints between the structure and the pontoons, high frequency waves are absorbed by the air-filled pontoons. The 2:1 length-to-beam ratio, in addition to the ball joint and suspension system, makes the WAM-V a stable platform (Marine Advance Research Inc. WAM-V). The WAM-V technology is modular. The entire vessel can be broken down into individual components that can be quickly replaced (Andrea A. Shen 2013). Figure 2.1 shows the dimensional layout (side and aft view) of WAM-V and the principal physical dimension of WAM-V used in this study is shown in Table 2.1.

Table 2.1 Main particulars of WAM-V

Parameters	**Measurements**
Hull Length	3.96 m.
Overall Vehicle Height	1.27 m.
Overall Vehicle Width	2.44 m.
Payload	136 Kg. (Maximum)
Full Load Displacement	255 Kg.
Draft	0.165 m.
Primary Sensors	GPS, Camera, LRF, INS, Hydrophone- Pinger

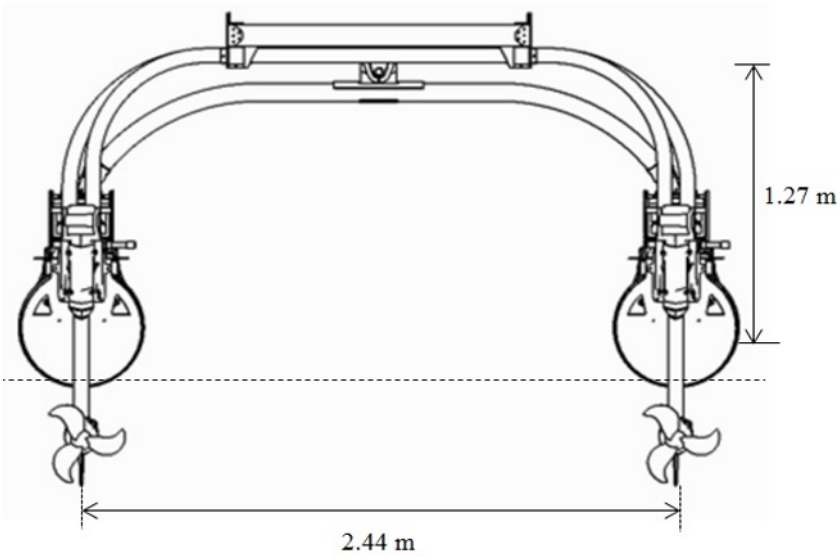

(a)

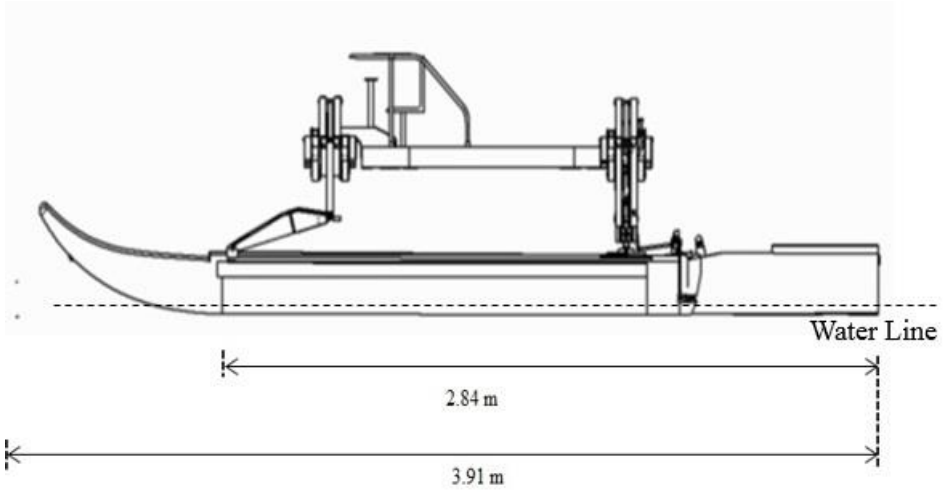

(b)

Figure 2.1 Dimensional Layout of WAM-V (a) aft view (b) side view(courtesy: RobotX Maritime Challenge)

2.2 ACTUATORS

The propulsion system of the vehicle consists of a pair of Minn. Kota transom mount trolling motors installed on the port and starboard side as shown in Figure 2.2. In

the original state of the thrusters, the RPM of the motor and its orientation are controlled by a foot pedal. The thrusters are custom designed in order to control it autonomously instead of pedal control. These electric thrusters are designed for 12 V, powered by 12 V deep cycle lead acid battery. The motor itself is sealed inside the compartment and it is submerged during the experiment which prevents overheating. The motor is controlled by Mbed NXP LPC 1768 microcontroller with H-Bridge module using RS 232 Serial port communication. The Mbed type of microcontrollers provides the fast and flexible type of platform and its online compiler is used to create motor control program. Minn. Kota thruster's specifications are given in Table. 2.2

Table 2.2. Minn. Kota Thruster Specifications

Parameters	**Measurements**
Propeller Type	Weedless Wedge
Number of the blades	2
Diameter	0.32 m

Figure 2.2 Minn Kota thruster (Courtesy: Minn Kota)

2.3 SENSORS

The vehicle features Furuno SC-30 Satellite compass, which provides highly accurate attitude information for navigation. The SC-30 consist of compact GPS antenna with a built- in processor. SC-30 Satellite GPS Compass Furuno Model used in this study is shown in figure 2.3, use NMEA 0183 protocol of communication. It delivers GPS position, heading, roll and pitch information, speed over ground (SOG), course over ground (COG) and rate of turn (ROT).

Table 2.3 SC-30 Satellite Compass Specifications

Parameters	Measurements
GPS Accuracy	10 m
Attitude Accuracy (Heading, Pitch & Roll)	0.50 rms
Heading Resolution	0.1 degrees

Figure 2.3 Furuno SC-30 satellite compass (Courtesy: Furuno)

2.4 ON-BOARD COMPUTERS

The hardware components comprising the Guidance, Navigation and Control (GNC) are located at the center of the hull. The main computer and various peripheral

devices, such as serial-to-USB interfacing hardware, voltage regulator, DC to AC converter and the wireless Local Area Network (LAN) hub, are housed in a sealed plastic fiber box.

2.5 POWER SUPPLY

The vehicle is powered by 3 G & Yuasa battery, SMF 27MS-730 (105Ah/20 hour rate capacity) batteries.

2.6 COMMUNICATION

WAM-V uses various sensors and actuators for its localization and actuation, each took in different communication protocols depending on firmware implementation, RS-232 communication, Controller Area Network (CAN), and USB protocols. Manual control of WAM-V is also possible via a wireless link, using a remote computer. Figure 2.4 shows the full hardware architecture of WAM-V. The propulsion module and sensor module interfaced with a high-level PC. The other PC is used remotely in order to control on board PC via the wireless network.

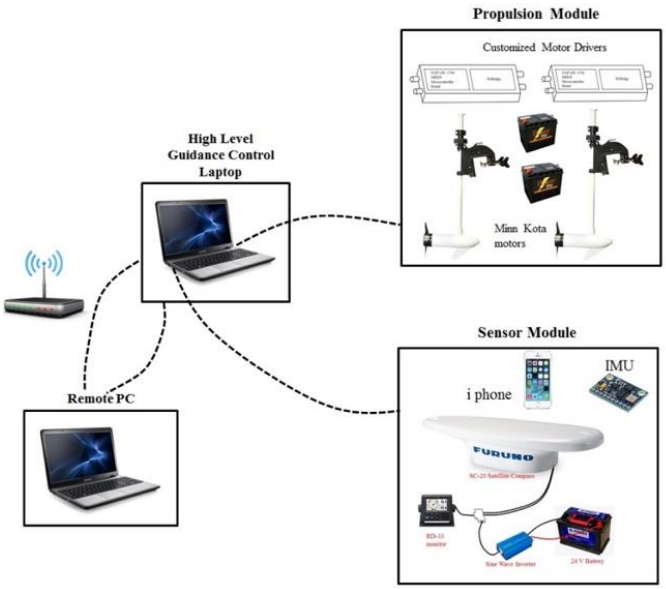

Figure 2.4 Hardware Architecture

2.7 SOFTWARE DESCRIPTION

The MATLAB/Simulink is used as a software platform in this research. The code for Mbed microcontroller is written in MBed firmware. The Mbed microcontroller can communicate with a host PC through a serial port. The interface program of motor driver and sensors are written in Matlab. Figure 2.5 (a) shows the control panel Graphical User Interface (GUI) for the free running experiments and (b) shows the control panel layout for waypoint navigation experiments.

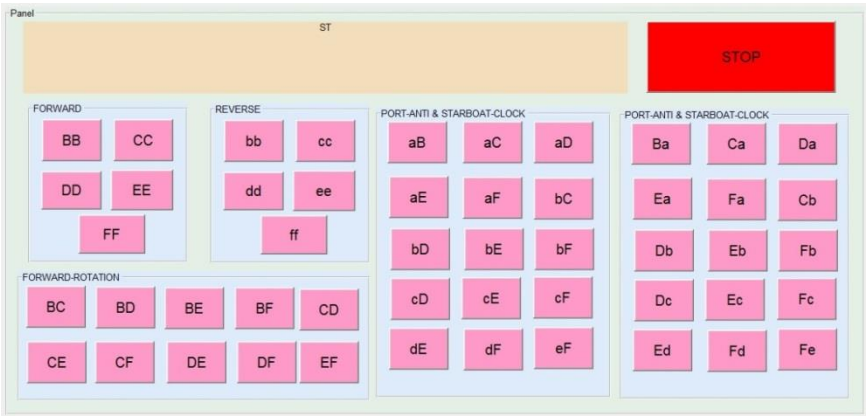

(a)

(b)

Figure 2.5 (a) GUI for manoeuvring experiments and (b) control panel GUI in Matlab for waypoint experiments

3. MATHEMATICAL MODELING

3.1 INTRODUCTION

A successful control system design requires knowledge of the system to be controlled. The mathematical model for ship manoeuvrability is the most important issue for a ship manoeuvring simulation. Numerous mathematical models were proposed to predict the ship manoeuvrablibity in the middle of the last century. A first zig-zag manoeuvre model was proposed by Kempf (1932) in which the manouevring motion and rudder action were established by applying a concept of control engineering in the zigzag manoeuvre. On the other hand, Davidson and Schiff (1946) developed the linear model of ship manoeuvring. Abkowits (1964 & 1980) has proposed one of the most extended non-linear mathematical models. Abkowits (1964) described the hydrodynamic force as a reaction forces to ship motion. In this model, the hydrodynamic parameters are expressed in the polynomial equation. The drawback of this model is up to which degree the polynomial equation should be extended to get the nonlinear effect, is difficult to analyze. Nomoto (1964) proposed first order mathematical model which is the simplest model to describe ship manoevres. This model used zigzag manoeuvring test data to calculate the manoeuvring indices (K & T).

Apparently, by the end of 1970's, many manoeuvring mathematical models were established. There is a well established MMG model proposed in the Japan Towing Tank Conference (JTTC) by Ogawa et al. (1977 & 1978). The model was proposed by a research group called Manoeuvring Modeling Group (MMG) (Yasukawa et al. 2015). The MMG model explicitly includes the individual open water characteristics of hull/propeller/rudder and their interaction forces. There are various advantages of MMG

type of mathematical model (Yasukawa et al. 2015) as described

1. Each Term of the model should be as much related to the physical meaning as possible.
2. Each term of the model should be in such a form as to allow easy evaluation by experiments.
3. Basic logical formulations should be framed into model for developing the model/full-scale correction method.
4. In consideration for design modification of the component configuration, such as the rudder, easier corrections of the hydrodynamic coefficients should be facilitated.

3.2 REFERENCE SYSTEMS

The MMG-type modular maneuvering model has been found to be suitable for investigation of maneuvering characteristics of the twin hull -twin propeller vessel. The model consists of a hull, propeller and rudder characteristics with their interaction effect. For the dynamic mathematical modeling of the WAM-V, several assumptions were adopted, namely, the WAM-V is assumed to be rigid and have a planar motion by neglecting heave, pitch and roll motion. For aquatic applications, WAM-V motion can be described by 3-dof which lies in the plane parallel to the surface of the water, namely surge, sway and yaw. The z-axis is chosen so as to be perpendicular to the x-y plane (positive downward). Figure 3.1 shows the Earth-fixed coordinate and body-fixed coordinate system of WAM-V.

Coordinate systems are defined for the control system design by $O - X_0Y_0$ (i.e, earth fixed coordinate system) and $G - XY$ (i.e., body fixed coordinate system). The

origin of the body-fixed coordinate is assumed to coincide with the center of gravity of WAM-V.

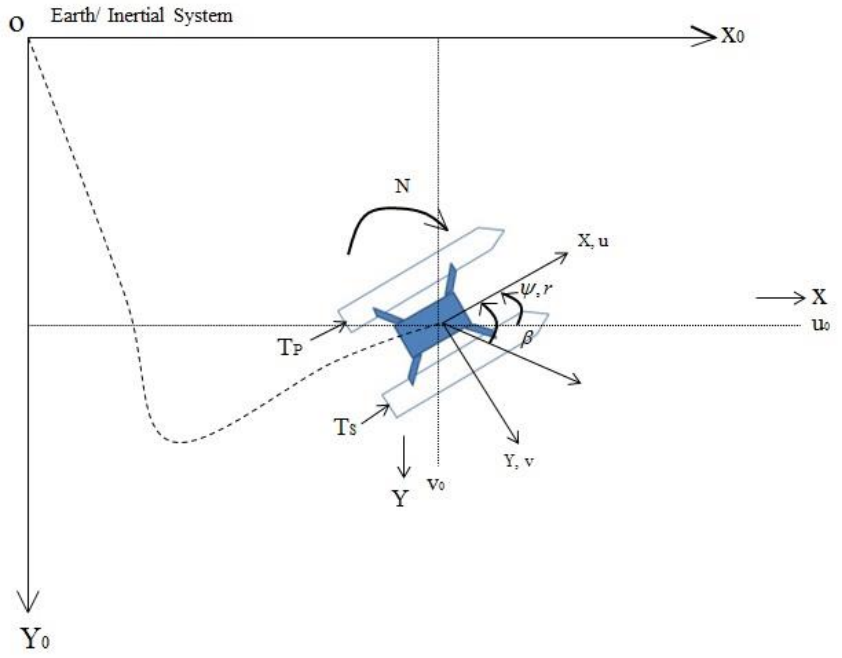

Figure 3.1 WAM-V Reference System

3.3 MODEL EQUATIONS

The non-linear dynamic equation can be expressed in vector form as given in equation (3.1) (Fossen 1994).

$$M\dot{\vec{\nu}} + C\left(\vec{\nu}\right)\vec{\nu} + D\left(\vec{\nu}\right)\vec{\nu} + G\left(\vec{\eta}\right) = \vec{\tau} \tag{3.1}$$

where M is the mass and inertia matrix (including added mass and inertia term), $C(\vec{\nu})$ is the centripetal and Coriolis acceleration, $D(\vec{\nu})$ is the hydrodynamic damping matrix, $G(\vec{\eta})$ is the restoring force and moment matrix, and $\vec{\tau} = [X, Y, Z, K, N, M]^T$ represents the resultant forces and moment matrix. WAM-V motion can be described by 3-dof which lies in the plane parallel to the surface of the water, namely surge, sway and yaw.

$$\begin{bmatrix} X \\ Y \\ N \end{bmatrix} = f\left(u, v, \dot{u}, \dot{v}, r, \dot{r}, n\right) \tag{3.2}$$

Based on the method of MMG, we can separately analyze the outside force and control force on the WAM-V, the equations of motions are shown in equation (3.3).

$$\begin{aligned} \left(m + m_x\right)\dot{u} - \left(m + m_y\right)rv &= X_H + X_P \\ \left(m + m_y\right)\dot{v} + \left(m + m_x\right)ru &= Y_H + Y_P \\ \left(I_Z + J_Z\right)\dot{r} &= N_H + N_P \end{aligned} \tag{3.3}$$

where u, v and r are vehicle's surge velocity, sway velocity and yaw rate respectively. m is the mass of the vessel. m_x and m_y are the added mass of ship in x- and y- directions respectively. I_Z is the moment of inertia about the z-axis. J_z is added mass moment of inertia of vessel with respect to z- axis. X_H , Y_H and N_H are the hydrodynamic forces acting on the hull. X_P, Y_P and N_P are the forces caused by WAM-V propellers. As there is no rudder, so rudder forces are zero. After expanding the equation (3.3) and putting the value of hull forces the Equation (3.4 a, b, c) is derived. The higher order terms (non- linear derivatives) are omitted.

$$\left(m + m_x\right)\dot{u} = X_u u + X_{uu} u^2 + X_{vr} vr + X_{rr} r^2 + X_{vv} v^2 + X_{uuu} u^3 \tag{3.4 a}$$

$$\left(m + m_y\right)\dot{v} + \left(m + m_x\right)ur = Y_v v + Y_r r + Y_{vvv} v^3 + Y_{vvr} v^2 r + Y_{vrr} vr^2 + Y_{rrr} r^3 \tag{3.4 b}$$

$$\left(I_Z + J_Z\right)\dot{r} = N_v v + N_r r + N_P \tag{3.4 c}$$

Initially, in order to increase the controllability of the vessel, the propellers are assumed to be turnable. The thrust is considered to be vectored in the X-Y plane. The motion of WAM-V is controlled by the revolution speed $n_{(P)}$ and $n_{(S)}$. The angles $\varphi_{(P)}$

and $\varphi_{(S)}$ of the two turnable propellers installed on the two hulls at the x_g distance from center of gravity G. The distance between the propellers action point and the baseline is y_p. The subscript (P) and (S) are defined as the port and starboard propeller, Figure 3.2 shows the schematic diagram of turning propeller arrangement of WAM-V.

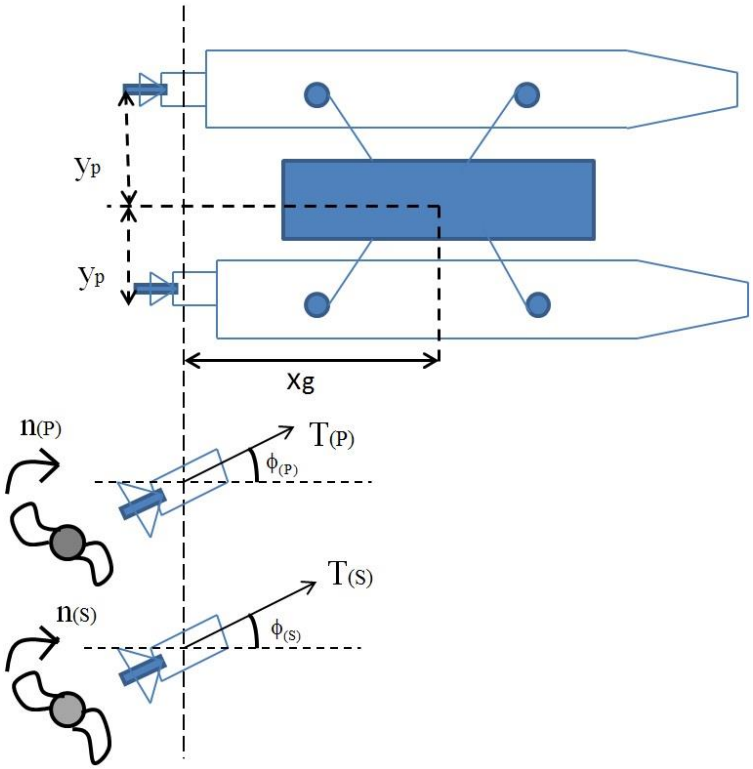

Figure 3.2 Schematic diagram of turning propeller arrangement of WAM-V

Equation (3.5) shows the propeller forces in x, y and z directions.

$$\begin{aligned} X_P &= X_{(S)} + X_{(P)} = (1-t_P)(T_{(S)}\cos\varphi_{(S)} + T_{(P)}\cos\varphi_{(P)}) \\ Y_P &= Y_{(S)} + Y_{(P)} = (1-d_{YP})(T_{(S)}\sin\varphi_{(S)} + T_{(P)}\sin\varphi_{(P)}) \\ N_P &= N_{(S)} + N_{(P)} = (1-d_{NP})(T_{(S)}(y_p\cos\varphi_{(S)} + x_g\sin\varphi_{(S)})) \\ &+(T_{(P)}(-y_p\cos\varphi_{(P)} + x_g\sin\varphi_{(P)})) \end{aligned} \tag{3.5}$$

Where t_p is the thrust deduction factor generated by the propeller in x-direction. d_{YP} and d_{NP} are the propeller influence factor to the Y and Z directions.

In case of fix propeller system $\varphi_{(P)} = \varphi_{(S)} = 0$. Y_P is theoretically zero. Hence, X_P and N_P expressions are derived as equation (3.6).

$$\begin{aligned} X_P &= (1-t_P)(T_{(S)} + T_{(P)}) \\ N_P &= (1-d_{NP})(T_{(S)} - T_{(P)})y_p \end{aligned} \tag{3.6}$$

In this case turning moment or rudder effect can be produced by generating differential thrust between the two propellors.

By eliminating v in equation (3.4b and 3.4c) and after non-dimensionalizing, the Nomoto's second order equation (3.7) for WAM-V can be derived as equation (3.7) - (3.16)

$$q1 \times \ddot{r} + q2 \times \dot{r} + q3 \times r = q4 \times P + q5\dot{} \tag{3.7}$$

$$q1 = (m + m_y)(I_Z + J_Z) \tag{3.8}$$

$$q2 = -Y_V(I'_Z + J'_Z) - N'_r(m' + m'_y) \tag{3.9}$$

$$q3 = Y'_V N'_r - N'_V(Y'_r - m') \tag{3.10}$$

$$q4 = N'_V Y'_P - N'_P Y'_V \tag{3.11}$$

$$q5 = (m' + m'_y)N'_P \tag{3.12}$$

$$P' = T'_{(P)} - T'_{(S)} \tag{3.13}$$

$$\dot{P}' = \dot{T}'_{(P)} - \dot{T}'_{(S)} \tag{3.14}$$

$$T'_1 T'_2 = \frac{q1}{q2}; (T'_1 + T'_2) = \frac{q2}{q3}; K_p = \frac{q4}{q3}; T'_3 = \frac{q}{q} \tag{3.15}$$

$$T'_1 T'_2 \ddot{r} + (T'_1 + T'_2)\dot{r} + r = K_p T' \dot{P}'_3 + K_p P' \tag{3.16}$$

Equation (3.16) can be regarded as the extension of 2nd order K-T equation proposed by Nomoto, which can be used in differential thrust condition. The difference between a traditional ship motion response equation and WAM-V motion is that the manoeuvre control variable is generated by the differential thrust, not by the rudder. Where the nondimensional parameters of K and T indices are shown in equation (3.17) and (3.18)

$$T' = \frac{TU}{L} \tag{3.17}$$

$$K' = \frac{KL}{U} \tag{3.18}$$

Where U is the forward speed of the vessel and L is the overall length of the ship.

Later on, it was realized that the only linear manoeuvring derivatives are not sufficient to describe the WAM-V dynamics because its dynamics is highly non-linear so it was decided to add some higher order manoeuvring derivatives. The 3rd order terms such as Y_{vvv} and N_{vvv} take into account as the values are already calculated from the drift captive model test, which is enough to guess for system identification calculation (Chapter 4). Whereas, Y_{vvr} and Y_{vrr} are neglected to reduce the complexities in identifying the other hydrodynamic parameters using system identification method (Chapter 5).

Equation (3.19), (3.20) and (3.21) describe WAM-V dynamic model including higher order derivatives.

$$m\left(\dot{u} - vr\right) = X_{\dot{u}}\dot{u} + X_{vv}v^2 + X_u\left(U\right) + X_P \tag{3.19}$$

$$m\left(\dot{v} + ur\right) = Y_{\dot{v}}\dot{v} + Y_{\dot{r}}\dot{r} + Y_v v + \left(Y_r + X_{\dot{u}}u\right)r + Y_{vvv}v^3 \tag{3.20}$$

$$I_Z\dot{r} = N_{\dot{v}}\dot{v} + N_{\dot{r}}\dot{r} + N_v v + N_r r + N_{vvv}v^3 + N_P \tag{3.21}$$

To simulate the manoeuvring motion, the manoeuvring derivatives in the equation (3.19-3.21) should be determined. Various studies were carried out to predict the manoeuvring derivatives for ship motion equations. Faltinsen (2005) performed his research on catamaran vessel and found that determining the hydrodynamic coefficients with the use of purely theoretical methods to predict the ship maneuverability is still underdeveloped. Although Inoue et al. (1981) derived some semiempirical formulae to calculate the manoeuvring derivatives of conventional ships. Motora (1959 and 1960) provided an empirical method for estimating the added masses and added moment of inertia from model tests with various conventional ships, which is known as Motora's chart. The WAM-V is neither similar to conventional ship nor like a usual catamaran vessel, so it doesn't satisfy the assumptions to use those empirical or semiempirical formulae. So it is decided to calculate the manoeuvring derivatives of WAM-V with the help of the captive model experiments and system identification method as described in Chapter 4. The calculated values from Captive tests is taken as the initial guesses in the system identification process. Certain parameters such as $Y_r, N_r, X_{\dot{u}}, Y_{\dot{r}}, N_{\dot{v}}$ and $N_{\dot{r}}$, which could not be determined from the captive model tests are estimated by means of the parameter identification methods.

4. MANOEUVRING IN CALM WATER

4.1 INTRODUCTION

International organization ITTC (International Towing Tank Conference) has developed a procedure of the model test and assessment of the manoeuvrability and performance of the ships (IITC, 1999). To study the manoeuvring behaviour of the ship, two fundamental testing methods, namely captive model tests and free running model tests are recommended. In captive model tests, manoeuvring hydrodynamic forces are measured by forced motion tests with a scale model. Contrarily, in the free running tests, a self-propelled model is steered by radio control or computer on-board in the basin. Some standard manoeuvers are proposed to check the adequate manoeuvrability of a ship such as speed test and turning test etc. (ITTC, 2011). In the recent year, due to a rapid development of the computer technology, computational fluid dynamic (CFD) simulation becomes more and more popular to study the ship manoeuvrability.

Two container ship has been used to study the turning circle behaviour and the manoeuvring behaviour is simulated by using 6 degrees of freedom of nonlinear mathematical models in regular waves (Fang et al. 2005). The hydrodynamic characteristics of Delft catamaran 372 were studied (Zlatev et al. 2009) both with the help of experiments and simulations, a good agreement was found between Experimental Fluid Dyamics (EFD) and CFD results. The manoeuvring performance of 3m ship was studied using free running, turning and zig-zag tests (Im et al. 2010). The model ship showed adequate manoeuvring characteristics and can be utilized for autonomous navigation tests. The prediction capability of manoeuvre behaviour using

EFD and CFD methods for tanker, container and surface combatant hull form were studied (Stern et al. 2011). The overall results show the comparative behaviour of free running tests using a variety of methods. The architecture description in terms of control, navigation and guidance of the Esso Osaka tanker model was described (Moreira et al. 2011). The manoeuvring tests were performed in calm water and the result confirmed the system performance characteristics which are acquired from simulations. The combined numerical and experimental method to determine the damping force and moment coefficients of a catamaran boat in calm water was presented (Hornaryar et al. 2014). The numerical results were found very close to experimental results. In order to calculate the hydrodynamic derivatives for DTMB 5512 model ship, CFD based virtual simulation was used (Ahmed et. Al 2015). The comparison of the simulated resource showed a good agreement with the experimental data, which give evidence that the CFD is precise and affordable tool at the preliminary stage. The MMG model has shown good results for manoeuvring in calm water (Ogawa et al. 1980). Yoshimura et al. (2015) revised the MMG mathematical model by adding some interaction coefficient in the model.

In this chapter, the captive model tests and free running tests are described briefly in order to study the manoeuvring behaviour of WAM-V.

4.2 CAPTIVE MODEL TEST

Captive model tests in towing tank are carried out using a planar motion mechanism (PMM) or a rotating arm. In a tow tank, the vessel is towed at different angles of attack, measuring sway force and yaw moment. Widely, there are three kinds of studies can be performed on a towing tank such as Open water tests (propeller),

Resistance tests (hull), Self- propulsion tests (hull and propeller). With these tests the actual hydrodynamic parameters of the ship can be calculated (Hirano & Takashima 2010).

In this study, only resistance tests and drift tests are conducted at Osaka University towing tank facility. The test basin is 100m in length, 7.8m in width and 4.35m in depth. The WAM-V is attached with the towing carriage (Fig. 4.2) that runs on two trails on either side. The carriage tows the WAM-V at different velocities. The load cell is mounted to the center of gravity of the WAM-V, which measures the force and moments of different tests. The schematic sketch of test setup is shown in figure 4.1. Figure 4.1 shows the schematic representation of the WAM-V during towing tank experiments.

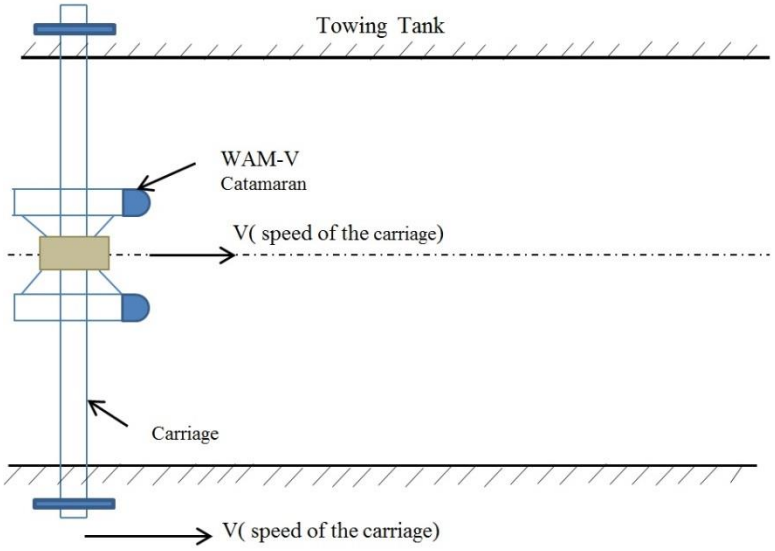

Figure 4.1 Schematic representation of towing tank setup

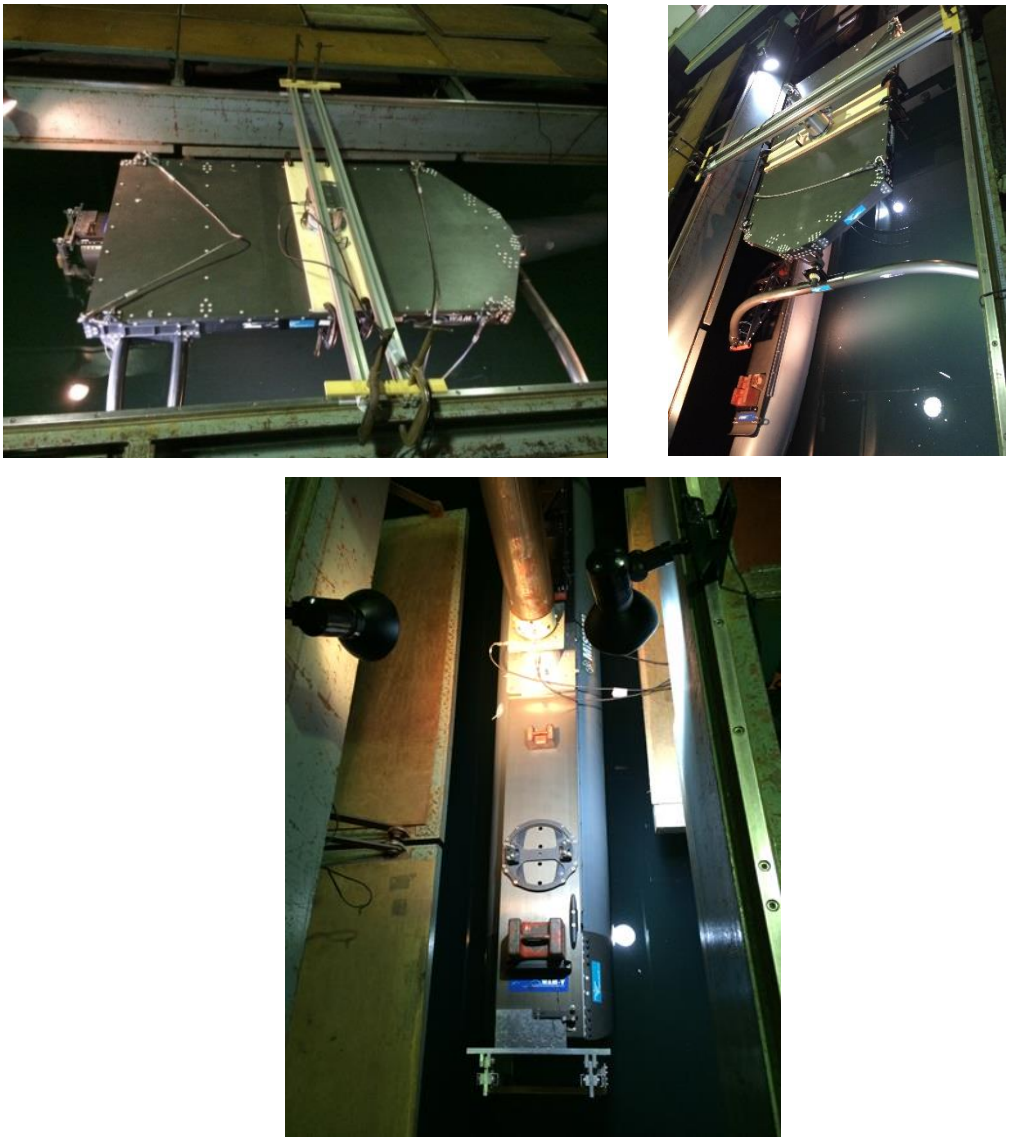

Figure 4.2 Experimental setup of towing tank experiments of WAM-V

The brief description of two tests conducted in this study is as follows:

1. Resistance Test:

An experimental study of a high-speed Delft catamaran vessel (Broglia et al. 2014) was conducted in order to investigate the hull interference effects on the total resistance advancing in calm water. The experiment was conducted at a different hull spacing (H/L, maximum is 0.30) and F_n (0.1-0.8). Where H is the hull separation distance and L is the length between the perpendicular. The result indicates the

difference in resistance between mono hull and the catamaran exists, ie. Interference effects have been always present. The resistance coefficient of the catamaran was found to largely exceed the corresponding value of the mono hull between F_n(0.35-0.7). The difference is, on the contrary less marked with the $F_n < 0.3$ as well as F_n >0.7.

In case of WAM-V, the hull spacing remained constant (ie. H/L=1.42). In this experiment, running attitude (trim and sinkage) is free. Table 4.1 shows the main flow parameters at experimental conditions. Figure 4.3 shows the resistance coefficient curve of full WAM-V and mono hull with respect to F_n

Total resistance coefficient C_t

$$C_t = \frac{R_t}{\frac{1}{2}\rho V^2 S} \tag{4.1}$$

Where R_t is the total resistance of the ship. V is the speed of the ship. ρ is the density of water. S is the wetted surface area of the ship. It can be observed from the experimental curve that at higher velocities (F_n >0.3) C_t for full catamaran is smaller than twice of the mono hull which is opposite to Delf catamaran. Hull separation distance may be one of the reasons.

Table 4.1 Main flow parameters computed at each experimental condition

F_n	U (m/s)	Re
0.037-0.388	0.200-2.401	$5.66 * 10^5$- $6.79 * 10^6$

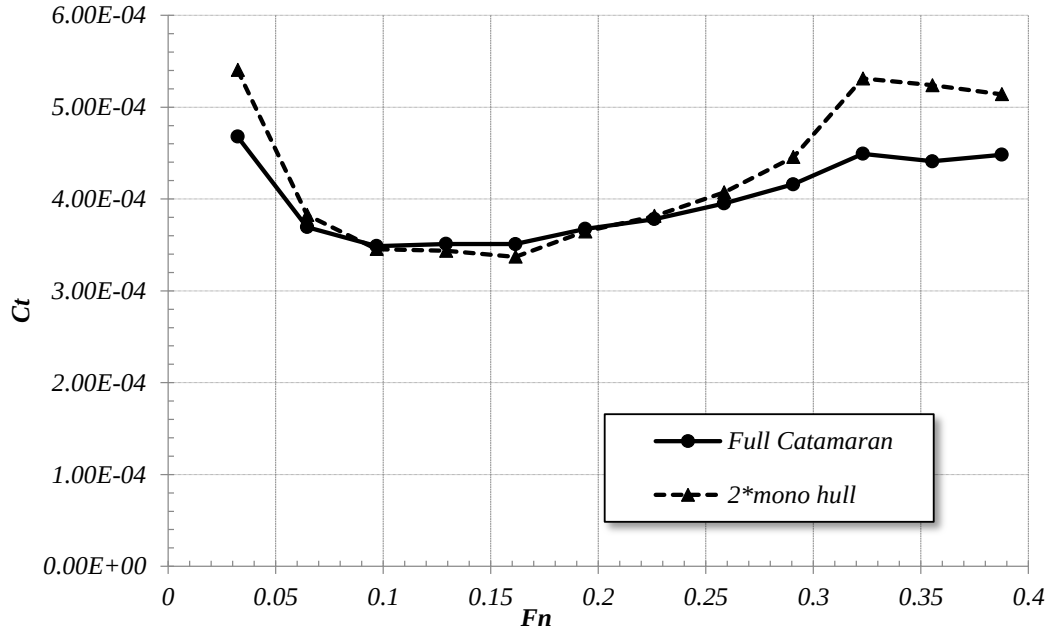

Figure 4.3 Resistance coefficient C_t as a function of Froud number F_n for full catamaran and twice of mono hull

2. Drift Tests:

In this test, Y_v ,Y_{vvv}, N_v and N_{vvv} at different angle of attack (β) is determined from the drift test. In this test the vessel is towed at a constant velocity, corresponding to a given ship F_n, at various β to the model path. The pitch and heave conditions are free. Equation (4.2) shows the relationship between angle of attack and velocity.

$$v = -V \sin \beta \tag{4.2}$$

where, the negative sign arises because of the sign convention adopted in this research. A load cell at the center of gravity, measures the force Y and yaw moment N experienced by the model at each value of β. The measurements are then plotted as a function of v (Fig. 4.5 and 4.6). The maximum capacity of load cell, used in the experiment is 490 N. Figure 4.4 shows the layout of experimental setup of drift test.

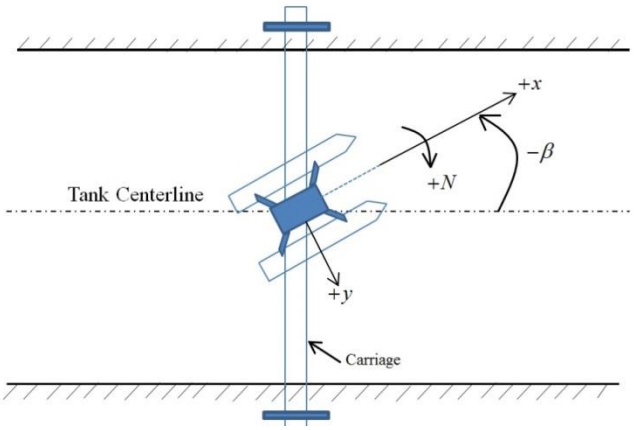

Figure 4.4 Orientation of model in the Towing Tank to determine Y and N

The figure 4.5 shows the relationship between the sway force (non-dimensional and vessel velocity (non-dimensional) at 1m/sec and 1.2 m/sec. Figure 4.6 shows the relational curve between yaw moment and vessel velocity at 1 m/s and 1.2 m/s. The drift angles varied from -15 degrees to +15 degrees at the step of 5 degrees. The gradient of the curve of force or moment versus velocity given the value of hydrodynamic derivatives ($Y_v, Y_{vvv}, N_v, N_{vvv}$).

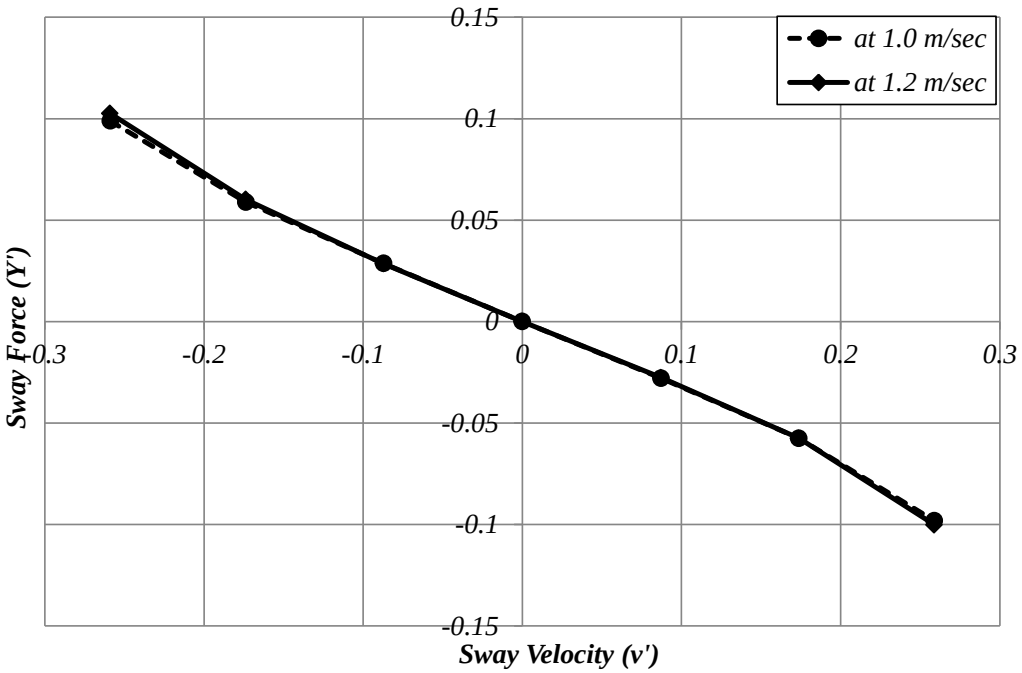

Figure 4.5 Non dimensional sway force vs non dimensional sway velocity

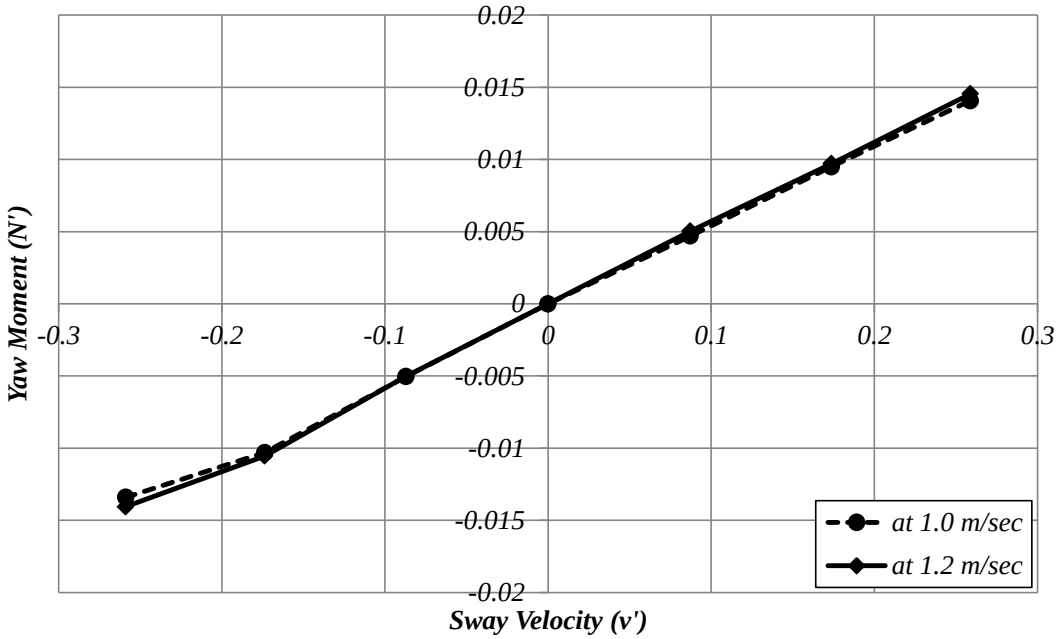

Figure 4.6 Non dimensional Yaw moment vs non dimensional Sway velocity

4.3 MANOEUVRING TEST

This kind of tests is the most direct method for predicting the manoeuvring performance. As it is described previously that there are two thrusters, to control the manoeuvrability of the WAM-V. The forward straight line motion can be achieved with the same forces generated by each thruster while turning manoeuvring can be achieved by differential thrust. Further, differential thrust can be achieved by two propeller rotation combinations, i.e. both the thruster rotating anticlockwise with same Revolutions Per Minute (RPM) and vice versa; the second case, both thruster have the same sense of rotation but different RPM. Figure 4.7 shows the four possibilities for the propeller rotation.

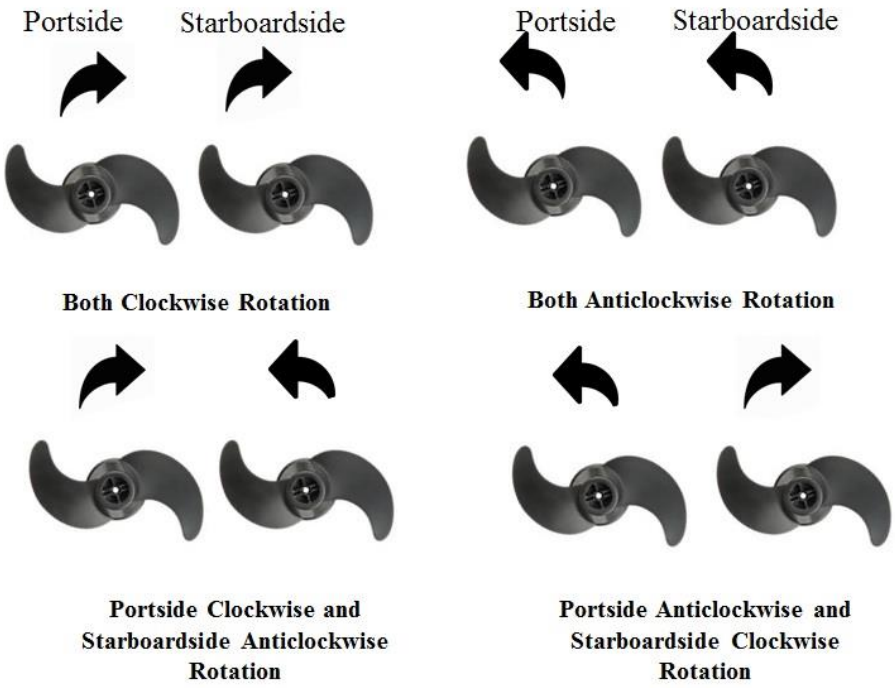

Figure 4.7 Different combinations of propeller rotation

In this research the thrusters are controlled by sending a Pulse Width Modulation (PWM) signal which means that the amplitude of voltage signal are controlled by user. The PWM signals vary from 0%-100% duty cycle. The 100 % duty cycle would be same as setting the voltage to 12 V. 0 % duty cycle would be same as grounding the signal.

In this free running experiments test the voltage signals are divided into 6 discrete values at the interval of 2.4 V. The symbolic notations for various combinations of voltage signals with the rotation direction are listed in Table 4.2

Table 4.2. Notations of control panel

Notation	Voltage (V)	Rotation Direction	Notation	Value	Rotation Direction
A	0	Anticlockwise	a	0	Clockwise
B	2.4	Anticlockwise	b	2.4	Clockwise
C	4.8	Anticlockwise	c	4.8	Clockwise
D	7.2	Anticlockwise	d	7.2	Clockwise
E	9.6	Anticlockwise	e	9.6	Clockwise
F	12	Anticlockwise	f	12	Clockwise

4.3.1 Speed Test

Speed tests are performed with the goal of identifying the relation between vehicle speed and voltage supplied. For the validation of the MMG mathematical model (Eq. 3.19-3.21) as described in Chapter 3, same set of voltage input as used for the straight line test was used as input for the MMG model to simulate and validate the dynamic behaviour of WAM-V. Figure 4.8 shows the block diagram of the MMG mathematical model developed in Matlab/Simulink to study the dynamic behaviour of WAM-V. The MMG mathematical model as described in Chapter 3 is used to simulate the dynamic behaviour of WAM-V with port and starboard side thrust as an input.

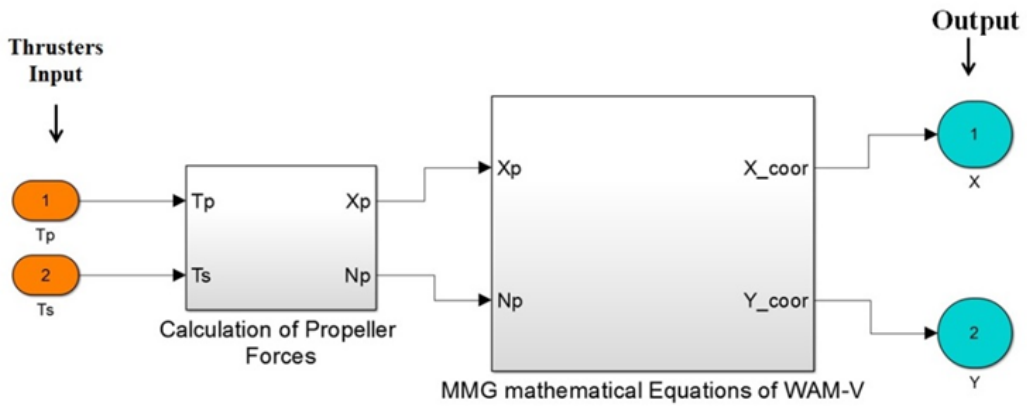

Figure 4.8 Block Diagram MMG mathematical model in Simulink

Figure 4.9 shows the relationship between the supplied voltage with respect to the speed of the WAM-V. For this experiment, the thrusters were supplied with different voltages such as 0V, 2.4V, 4.8V 7.2V 9.6V & 12V and the corresponding speed was measured when the WAM-V achieved steady-state condition. The solid line in the plot (Fig. 4.9) shows the experimental result and the dotted line shows the simulation results derived using MMG model. From the Fig 4.9 it can be concluded that the MMG model (Equation. 3.18-3.21) is good enough to reproduce the experimental results using the same set of input voltage

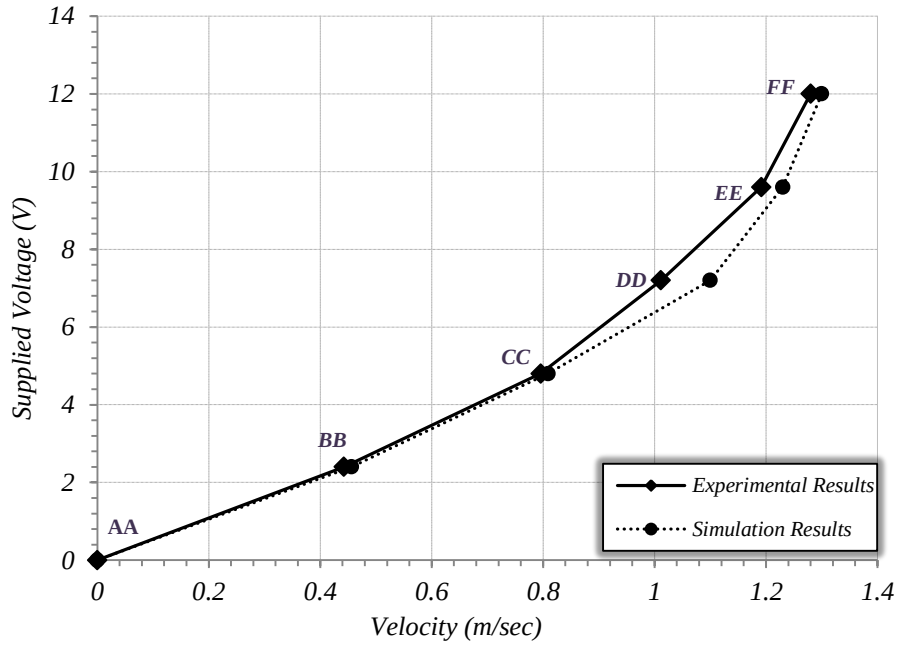

Figure 4.9 Experimental and simulation results of speed test

The relationship between voltage and thrust generated by the propeller is discussed in the next section.

4.2.3 Thrust Measurement

In this research the thrust generated by the propellers is calculated indirectly. In section 4.2 of this chapter, the resistance of WAM-V at a different vessel velocity is measured with the help of the captive model resistance test. From the captive model resistance test it can be concluded that resistance (R) is a function of vessel velocity (v) (Equation 4.3).

$$R \propto f_1(v) \tag{4.3}$$

Similarly from the free running experimental result, it can be shown that the input voltage (V) to the thruster is a function of v (Equation 4.4)

$$V \propto f_2(v) \tag{4.4}$$

Hence, from the equation (4.3) and (4.4), the relationship between (R) and (V) can be written as per equation (4.5).

$$V \propto f_3(R) \tag{4.5}$$

Finally, following the same formulation as explained above the relationship between input voltage (V) and Thrust (T_P, T_S) can be derived. The resistance force (R) and supplied voltage (V) are plotted with respect to the vessel velocity (v) in Fig. 4.10.

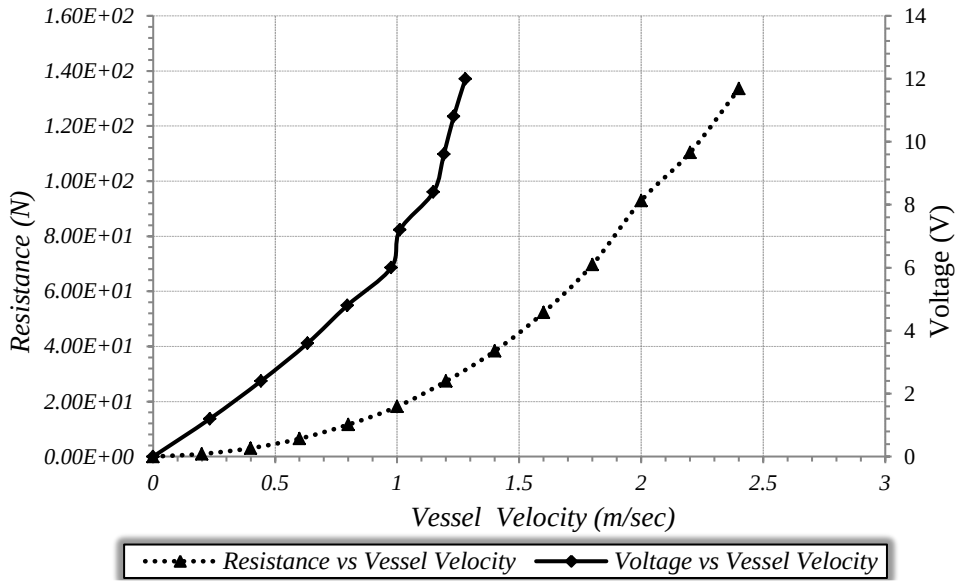

Figure 4.10 Ship resistance vs vessel velocity (solid line) and input voltage vs vessel velocity (dotted line)

From the above graph, with the same vessel velocity, thrust and voltage value can be obtained which is shown in Figure 4.11. This relation is used to determine the turning test input (Thrust) and lookup table which is described in chapter 7.

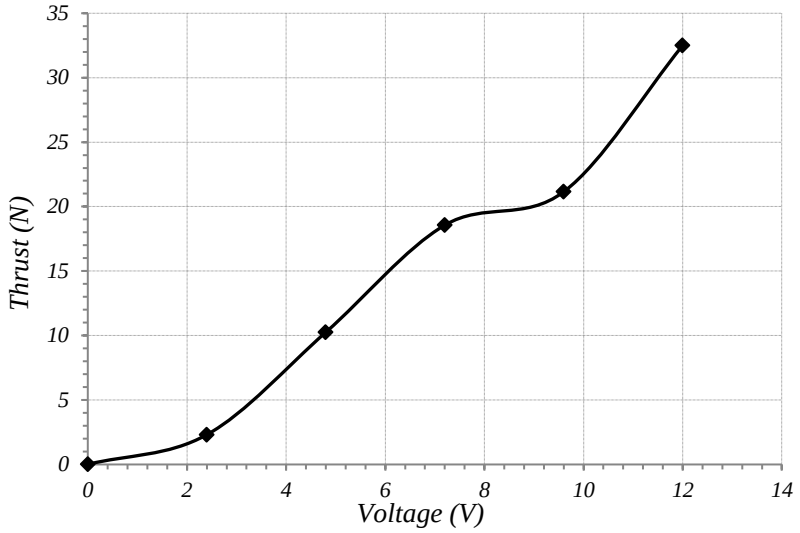

Figure 4.11 Propeller thrust vs voltage plot

4.3.2 Turning Test

In order to study the turning behaviour of WAM-V for various differential thrust combinations as defined in Table 4.2 turning test experiments were conducted. Thruster rotation speed and direction of rotation both governs the turning behaviour of WAM-V. Hence two sets of experiments were designed to study turning manoeuvring characteristics of WAM-V.

Turning Experiment 1: Sense of rotation of both the propellers is different

In this type of experimental tests, the port side propeller and starboard side propeller rotation directions are set to be different. Figure 4.12 shows the experimental trajectories of various turning tests For example, in the case of Fb test, the port side propeller is rotating anticlockwise direction with 12 V and a starboard side propeller is rotating clockwise direction with 2.4 V. In every experimental case the corresponding GPS position was recorded and plotted offline. Due to same pitch propellers used on port and starboard side, there is some discrepancy in port side and starboard side turning which is evident in turning plot. In this experiment, the wind condition was not

measured.

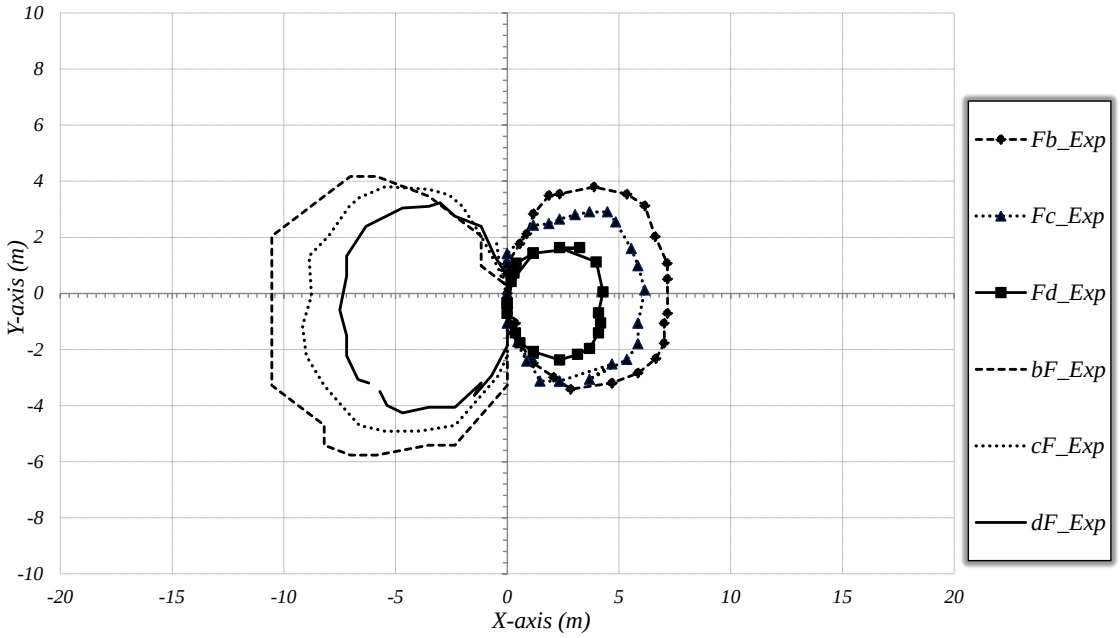

Figure 4.12Turning trajectories of WAM-V on port side and starboard side with different rotation direction of the propellers

Turning Experiment 2: Sense of rotation of both the propellers are same

For this type of experimental tests, the port side propeller and starboard side propeller rotation directions are taken anticlockwise, but voltage supplied to each propeller is different. As the clockwise sense of rotation gave reverse motion. Figure 4.13 shows the trajectory plot of turning test. The graph shows the trajectory of BD test which means the port side propeller is turning in anticlockwise direction with 2.4 V and starboard side turning is also anticlockwise with 7.2 V.

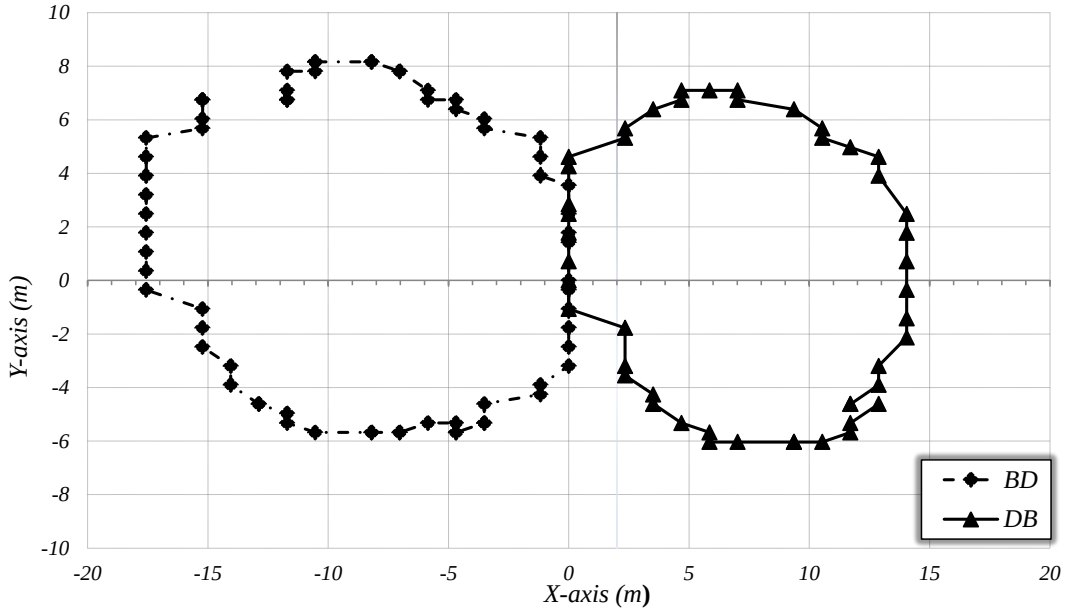

Figure 4.13 Turning trajectories of WAM-V on port side and starboard side with same rotation direction of the propellers

The left hand side and right hand side trajectories of experiment results may have some effect of different wind conditions. Hence, the controlled voltage of port and starboard side thruster can produce similar manoeuvering forces as that of conventional rudder. In order to better quantify the vehicle dynamics, these experimental studies have enabled significant advances in the understanding of high-speed vehicles like WAM-V. The use of free running models also provides the opportunity to test in open water conditions, which not only reduces reliance on high-cost test facilities but is also of particular importance for high-speed crafts. The assessment of system failure conditions in practical situations on WAM-V designs has also been the feature of the free running test.

5. SYSTEM IDENTIFICATION

In this chapter, the process and results of system identification method for WAM-V are described. The list of all the manoeuvring derivatives calculated with the help of captive model tests and system identification method for WAM-V is presented.

5.1 INTRODUCTION

A system identification approach is useful in providing reliable and accurate models in a short time. In system identification, input and output signals from the experiments are recorded and subjected to data analysis in order to infer the model. The simulation data do not match with measured data because the parameters are incorrect. There are some values, which are unmeasured and couldn't tune manually to match the results. However, using an optimization algorithm, these parameters can be automatically tuned until the result of the simulation match the measured data. The layout of system identification is shown in Figure 5.1. In this figure, u is the measured input and z is the measured output. y is the predicted output. The objective of identification is to minimize the error $(z - y)$. The estimation procedure is repeated process until process and model is successfully matched. System identification generally consists of the following four steps (Naeem, Sutton and Chudly 2003).

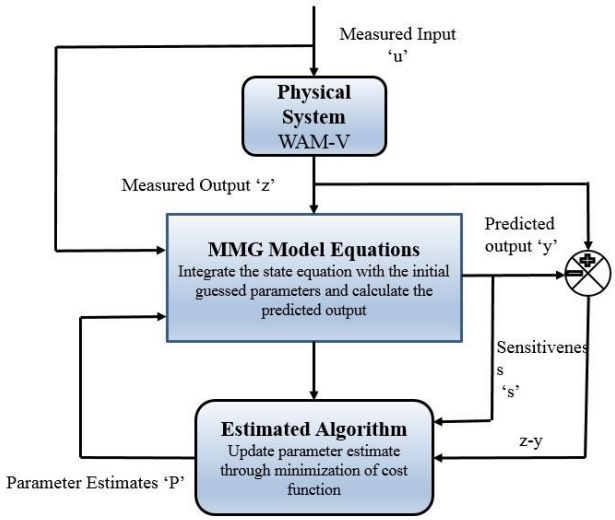

Figure 5.1 System Identification Layout

1. Data acquisition: First step is to obtain input/output data of the system to be identified. The data should be accurate enough to simulate the results.

2. Characterisation: The second step is to define the structure of the system.

3. Identification/estimation: The third step involves identifying the parameters by some initial guesses and define their ranges.

4. Verification: The final step is to identify the model response and cross validate with the other experimental results.

As Ljung (1999) explained in a synopsis about the system identification technique, including various parameter estimation methods. An introduction to the subject of system identification (Ljung 1999) divides a vehicle modeling techniques into the three Categories, first is a white box model, which is based on the principles of physics and empirical knowledge. The second is a black box model, which employs methods that make no assumptions about the system and third is the combination of above two is called grey box. Observer/ Kalman IDentificatin (OKID) theory was used to generate a system model of wing-sail catamaran 'Atlantis', (Elkaim 2001) and

(Elkaim and Parkinson 2008). With this model, Linear Quadratic Gaussian (LQG) controllers were simulated, which demonstrated excellent line tracking performance. A model of an AUV was developed with a practical system identification method using input/output data of experiments and tested in simulation using Linear Quadratic Gaussian (LQG) controller (Naeem et al. 2003). The dynamic model of USV 'Springer' was obtained using system identification and system model was used to simulate the control performance (Naeem et al. 2006). Caccia et al. (2008) developed the practical model and corresponding identification procedure for guidance and control of an autonomous surface craft (ASC) name Charlie. used the Observation Kalman Identification (OKID) method for identifying a linear time invariant plant model of a catamaran vessel. Oh, et al. (2010) described a mechatronic system for a model ship in order to get the manoeuvring data. The manoeuvring parameters were calculated with the help of the data using system identification technique ad mathematical model was developed. Wirtensohn et al. (2013) estimated the parameters of USV 'CaRoLIME' using a weighted least square optimization approach. Several manoeuvre trials were performed to gather the data as an input and output to the system identification toolbox.

5.2 PARAMETER ESTIMATION

In this research parameter estimation toolbox of Matlab is used to calculate the manoeuvring parameters of MMG model. The estimation method is chosen as Auto-Regressive model with eXogenous variables (ARX) model. ARX is an efficient polynomial estimation method, which uses nonlinear regression equations in analytical form. The nonlinear ARX model computes the output in two stages. In the first stage, it computes regressor values from the current and past input value and past output data.

After that, it maps the regressors to the model output using the nonlinearity estimator block equation (5.1)

$$y_p(t) = F(y(t-1), y(t-2), y(t-3), ..., u(t), u(t-1), u(t-2), ..) \quad (5.1)$$

Where u, v, and y are the input, output and noise correspondingly. For the approach to parameter identification, a minimum of two different data sets is required, one to determine the unknown parameters and other for the validation or vice versa. Unfortunately, identifying system parameters of the tests is not trivial. In this research, several data sets are used to get the best possible set of parameters. Although experimental data are sometimes unusable due to low sensor resolution. Thus, it is necessary to find an alternative to calculate estimated parameters. The alternative way is to create the data by creating mathematically-based computer simulation model with known parameters determined from the literature.

In this research, numerous speed tests and turning tests experimental data are used for simulation. We need to estimate the optimum parameters for the MMG type mathematical model of WAM-V. Therefore the model should be as accurate enough to simulate the parameters. Figure 5.2 shows the WAM-V mathematical model developed in Simulink (Equation 3.15-3.17). There are two inputs in the form of the port, starboard side thrust and two outputs as X and Y values of vessel's trajectory.

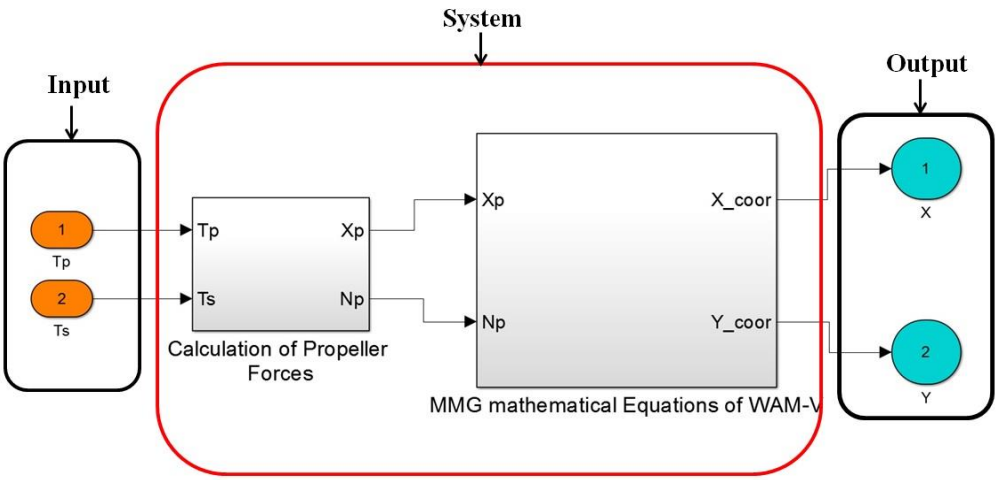

Figure 5.2 WAM-V mathematical model in Simulink

Figure 5.3 (a) shows the results of experimental 1. In this test, input conditions are $T_S = 18.56\,N$ and $T_P = 2.3\,N$. Simulated trajectory tries to best fit with measured trajectories (X and Y) by calculating the set of unknown parameters. The same set of parameters is kept constant in order to verify with experiment 2 data. Figure 5.3 (b) shows the result of experiment 2, where T_S =32.5 N and T_P =2.3 N is the input condition. In experiment 2, data are simulated to verify the same set of parameters in different thrust input as a result best fit simulated data is achieved. In this research, simulation with several combinations of different input-output conditions using the same parameter value are performed in order to check the accuracy of the estimated parameters.

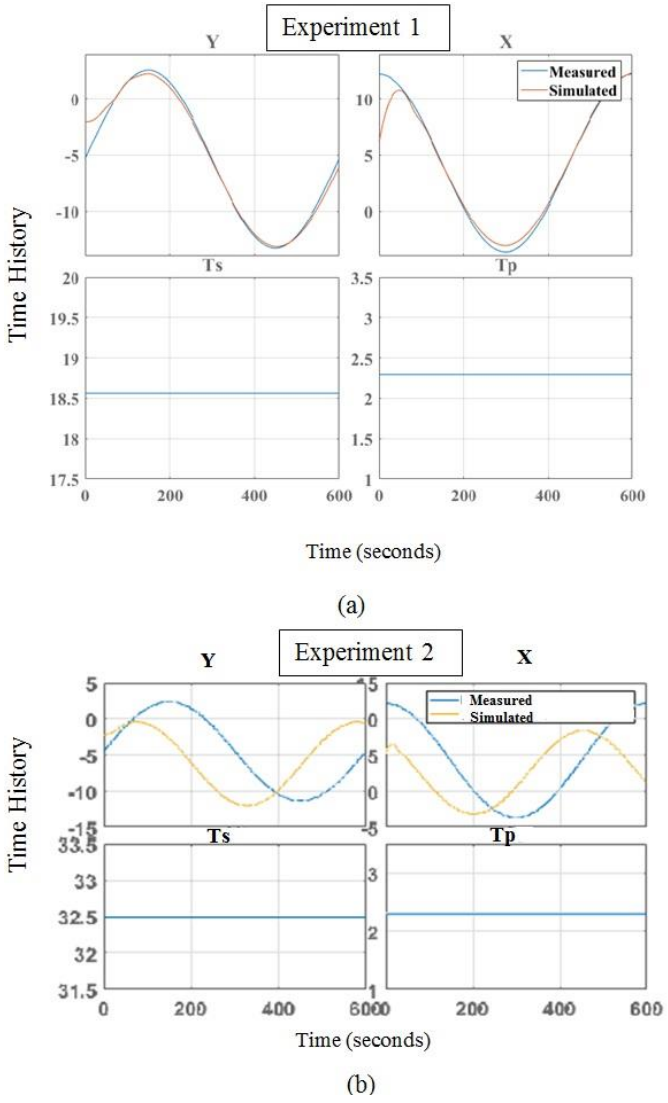

Figure 5.3 (a) Measured and simulated results of data set 1. (b) Validation of the same parameters with dataset 2

Figure 5.4 shows the measured (from experiments) and simulated turning trajectories of experiment 1 and experiment 2. Unknown manoeuvring derivatives are calculated with the help of experiment 1 and with the same manoeuvring parameters using experiment 2 data is simulated, which validates the values of calculated manoeuvring derivatives. Due to different initial conditions there is some phase shift in the trajectories.

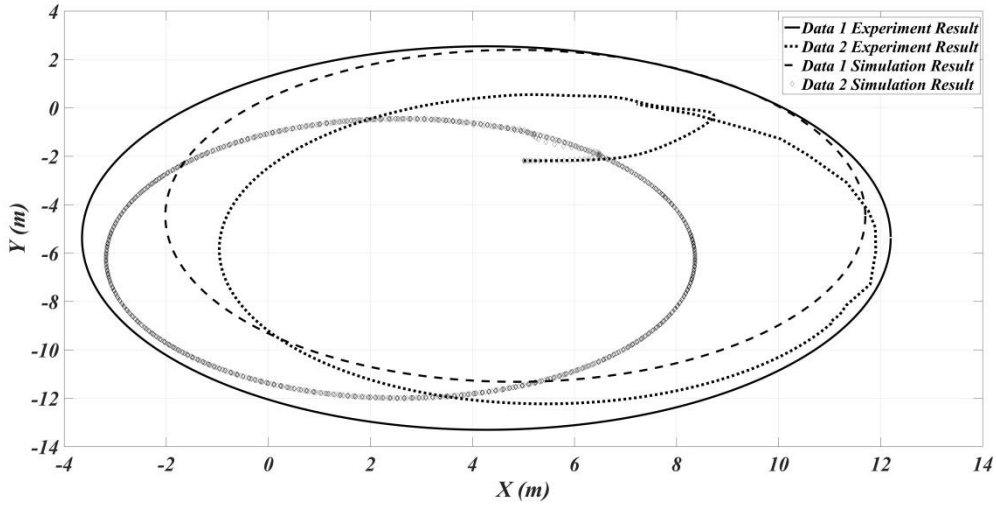

Figure 5.4 Measured and simulated turning test results with validation results

The dynamic of WAM-V is very complex, so many of the parameters are not so accurately estimated in every simulation. Only less erroneous data are simulated to get the maneuvering derivatives. Figure 5.5 shows the time history of estimated parameters. The final values of manoeuvring derivatives calculated with the help of system identification method are listed in Table 5.1.

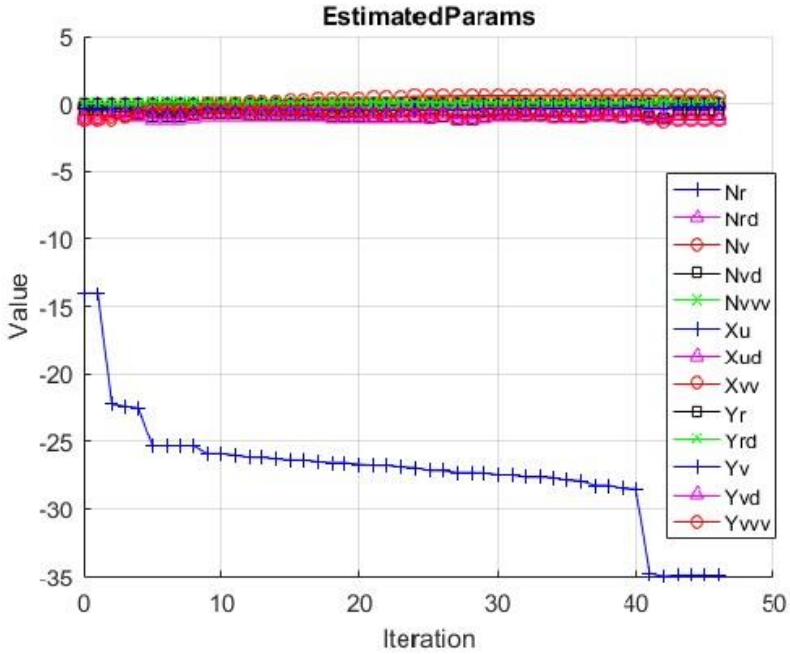

Figure 5.5 Time history of estimated parameters

Table 5.1. Calculated Manouevring Derivatives

Derivatives	Non-dimensional	System Identification Data Magnitude (non-dimensional) *10e-3
$X_{\dot{u}}'$	$\frac{X_{\dot{u}}}{1/2\,\rho L^2 d}$	-840
X_{vv}'	$\frac{X_{vv}}{1/2\,\rho L d}$	-880
$Y_{\dot{v}}'$	$\frac{Y_{\dot{v}}}{1/2\,\rho L^2 d}$	-1120
$Y_{\dot{r}}'$	$\frac{Y_{\dot{r}}}{1/2\,\rho L^3 d}$	-435
Y_{v}'	$\frac{Y_{v}}{1/2\,\rho L d U}$	-1155
Y_{r}'	$\frac{Y_{r}}{1/2\,\rho L^2 d U}$	-500
Y_{vvv}'	$\frac{Y_{vvv}}{\rho L d / 2U}$	-0.80
$N_{\dot{v}}'$	$\frac{N_{\dot{v}}}{1/2\,\rho L^3 d}$	25
$N_{\dot{r}}'$	$\frac{N_{\dot{r}}}{1/2\,\rho L^4 d}$	-89
N_{v}'	$\frac{N_{v}}{1/2\,\rho L^2 d U}$	-265
N_{r}'	$\frac{N_{r}}{1/2\,\rho L^3 d U}$	-177
N_{vvv}'	$\frac{N_{vvv}}{\rho L^2 d / 2U}$	1659

The draft (d), the length of the ship (L) and mass (m) are already described in Table 2.1. The values of $X_{\dot{u}}{}'/_m$ 0.05321 and $Y_{\dot{v}}{}'/_m$ are 0.32. The methodology to calculate the unknown hydrodynamic parameters of MMG model, which is difficult to calculate with the help of captive model tests is discussed in this chapter. While it was not possible to conduct the complicated experiments to calculate unknown manoeuvring derivatives for WAM-V, system identification method is one of the powerful optimization tools.

6. FUZZY WAYPOINT ALGORITHM

This chapter introduces the fuzzy reasoned waypoint algorithm which is used as a guidance system for autonomous waypoint navigation of WAM-V. The fuzzy control rules, a membership function with the fuzzy reasoning is briefly described in this chapter.

6.1 BACKGROUND

Waypoint Guidance is very useful for terrestrial navigation, air navigation and ocean navigation. Waypoint Guidance uses potential information obtained from positional sensors. Using the waypoint information, the path of the vessel is defined. In the mathematical view, the path can be defined as a continuous function. There are many ways to track the path. Although there are various control techniques for waypoint navigation are available in the literature but most of them are based on modern control theory. Fuzzy logic control is a practical alternative for a variety of challenging control and guidance problems. It shows an advantage over conventional autopilot because it is robust and guarantees the optimality of the system performance. According to Amerongen et al. (1977), fuzzy is an effective alternative approach for the system which is difficult to model and after that first autopilot design with fuzzy set theory was developed.

Cheng and Yi (2006) developed double loop fuzzy autopilot for waypoint tracking control in which the inner loop deals the ship course control and the outer loop deals the tracking control. Oh, and Sun (2010) presented the model predictive control (MPC) scheme using line of sight (LOS) algorithm for underactuated marine surface

vessels. Jia et al. (2012) developed the fuzzy switched PID controller for ship track keeping in which the fuzzy PD controller is used for improving the response, reduce overshoot time and fuzzy PI controller is used for improving the accuracy. Ahmed and Hasegawa (2016) presented the simulation and experimental results of the fuzzy waypoint guidance algorithm for Esso Osaka Ship and showed the promising experimental and simulation results in the research.

6.2 ALGORITHM DESCRIPTION

A waypoint guidance algorithm based on fuzzy logic mimic a human heuristic knowledge to control the ship. The waypoint heading guidance algorithm is realized by fuzzy control methods used for Ship Auto-Navigation Fuzzy Expert System (SAFES) (Hasegawa et al. 1986). The desired heading commands targeting two waypoints at one time is generated by the analysis of fuzzy logic.The fuzzy reasoning algorithm will decide the appropriate course define by the next two waypoints as given in Equation (6.1).

$$\psi_d = \psi_1 + (\psi_2 - \psi_1) * CDH \tag{6.1}$$

Where ψ_d is the order of course and ψ_1 is a course of the shortest path to the next waypoint, ψ_2 is the course of the shortest path to the second next waypoint. Correction for a degree of heading (*CDH)* is reference degree to the second waypoint (0≤CDH≤1). In this algorithm, to judge the nearness of the waypoint, *TCPA* (time to closest point of approach) and *DCPA* (distance of the closest point of approach) are used for fuzzy reasoning. If *DCPA* is very big and *TCPA* is also very big, then *CDH* is very small. Which shows that the ship is far from second waypoint then the command course will target only for the first waypoint. As the values of DCPA and TCPA are decreasing

the ship is reaching closer to the first WP. The algorithm is described step by step in detail below.

At first the waypoints (WP) are initialized as $W_i = (X_i, Y_i)$, $W_{i+1} = (X_{i+1}, Y_{i+1})$ and current vehicle position (P) and vessel heading ψ is obtained from the sensor.

The distance between the ship and nearest waypoint (D) is calculated by equation (6.2)

$$D = \sqrt{(X_0 - X_t)^2 + (Y_0 - Y_t)^2} \tag{6.2}$$

Encountering angle of waypoint from the vertical axis (θ) and bearing angle of waypoint (α) from the ship are calculated with the help of equation (6.3) & (6.4) Here, if the value of ψ, θ or α becomes negative, then 2π is added to make them positive.

$$\theta = a\tan 2\frac{(Y_t - Y_0)}{(X_t - X_0)} \tag{6.3}$$

$$\alpha = \theta - \psi \tag{6.4}$$

Figure 6.1 (a) shows the course changing command near a course changing point (WP) and (b) shows the bearing relationship between the ship and waypoint. *TCPA* and *DCPA* are calculated with the help of equation (6.5) & (6.6).

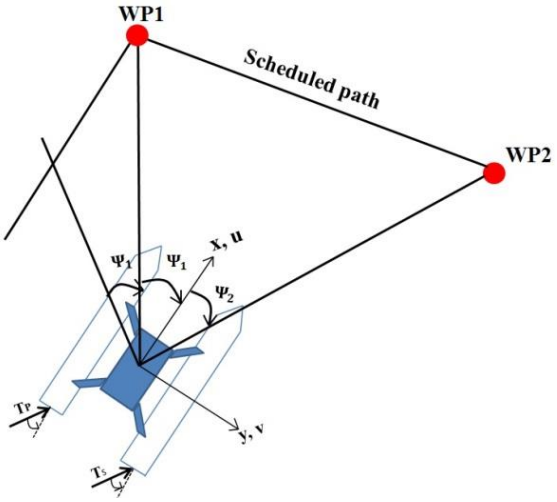

(a)

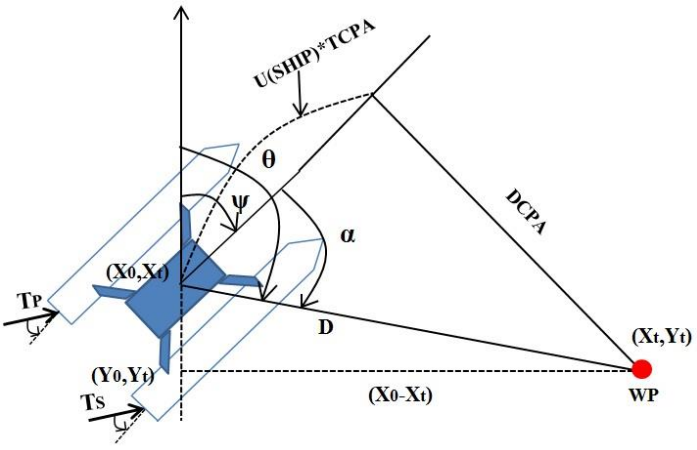

(b)

Figure 61 (a) Course command near a course changing point (b) Bearing relationship between ship and waypoint

$$DCPA = D\left|D\sin\alpha\right| \tag{6.5}$$

$$TCPA = \frac{D\cos\alpha}{U_{ship}} \tag{6.6}$$

Another important point to be considered is the scale effect. There should be some difference on the nearness between a large ship and a small one. Therefore, the following equations are used for non-dimensionalised *TCPA* and *DCPA*. The nearness is

then reasoned with $DCPA'$ and $TCPA'$ instead of $DCPA$ and $TCPA$ using the Equation (6.7) & (6.8) is calculated.

$$DCPA' = \frac{DCPA}{L} \tag{6.7}$$

$$TCPA' = \frac{TCPA}{L/U} \tag{6.8}$$

When the $TCPA'$ becomes negative the waypoint is switched and next set of waypoints is targeted. The nearness of the waypoint is identified using fuzzy logic by calculation $TCPA'$, $DCPA'$ and CDH, which is discussed in the next section. The waypoints are stored in the form of GPS location and are used to generate the desired trajectory to follow.

6.3 FUZZY REASONING

Fuzzy logic controller mimics human reasoning and logic by developing sets of distributive membership functions (Driankov et al. 1996). The fuzzy controller block diagram is given in figure 6.2. There are two crisp inputs in the form of the $\mathrm{TCPA}'$and DCPA'. The experience of human heuristic knowledge is explicitly integrated into the control rules of the fuzzy logic in order to take the decision. The minimum-maximum method is utilized to obtain the fuzzy value. The fuzzy output set is defuzzified using the center of gravity (COG) method. Finally, CDH is calculated as a crisp output.

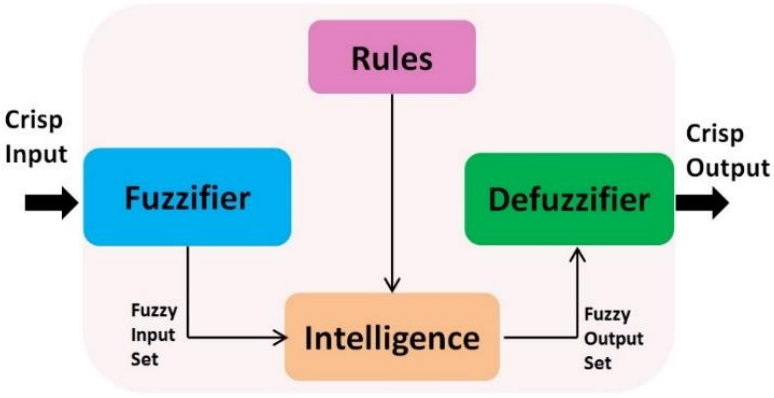

Figure 6.2 Fuzzy Controller Architecture

The linguistic variables are defined as:

$TCPA'$ = {SA, SM, ME, ML, LA}

$DCPA'$= {SA, SM, ME, ML, LA}

CDH= {SA, SM, ME, ML, LA}

Where SA= SMALL, SM= SMALL MEDIUM, ME=MEDIUM, ML=MEDIUM LARGE, LA=LARGE.

The complete fuzzy system implicates 25 fuzzy rules with 5 linguistic variables. The triangular membership functions of $TCPA'$, $DCPA'$ and CDH is shown in Figure 6.3. The fuzzy control rules to reason CDH with the help of $TCPA'$ and $DCPA'$ is shown in Table 6.1.

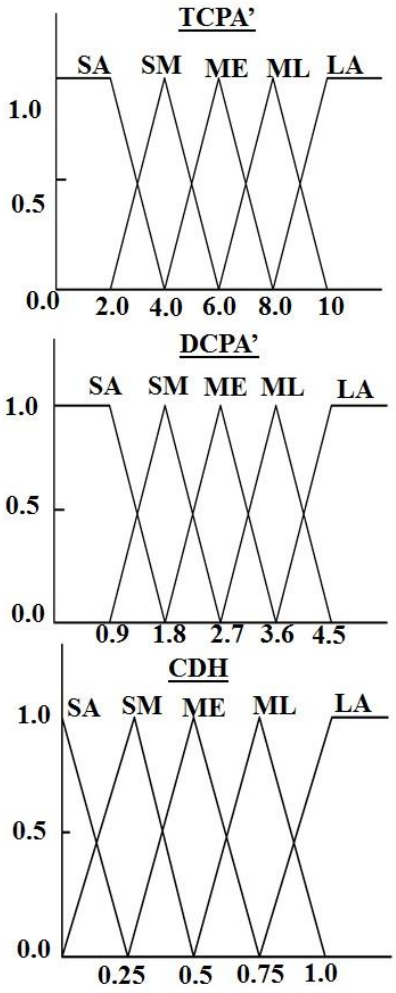

Figure 6.3 Membership functions for course changing algorithm

Table 6.1 Fuzzy Control Rules

		$TCPA'$				
$DCPA'$		SA	SM	ME	ML	LA
	SA	LA	ML	ME	SM	SA
	SM	ML	ME	SM	SA	SA
	ME	ME	SM	SA	SA	SA
	ML	SM	SA	SA	SA	SA
	LA	SA	SA	SA	SA	SA

Defuzzification is the process of converting degree of membership of the output linguistic variable into numerical values. There are various methods such as the center

of area (COA), Center of Sums (COS) or Center of Maximum (COM) etc. In this research Center of Gravity (COG) method is used (Mamdani 1974). Equation (6.9) shows the function equation and figure 6.4 shows the graphical representation of the COG function.

$$y' = \frac{\int_Y \mu(y)\, y dy}{\int_Y \mu(y) dy} \tag{6.9}$$

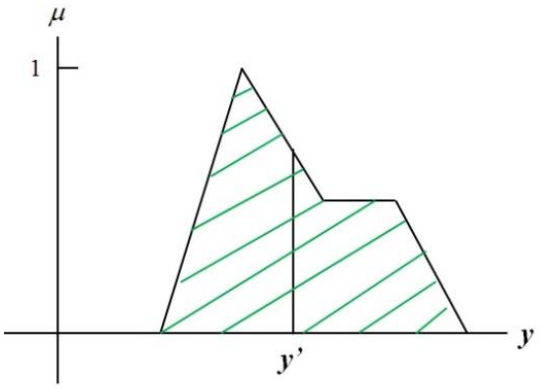

Figure 6.4 Center of Gravity Function

which chooses the y -coordinate of the center of gravity of the area below the graph μ (y). This defuzzification can be interpreted as a weighted mean, i.e. each value y is weighted with μ (y) and the integral in the denominator serves for normalization.

The characteristics of the fuzzy control surface, that is a graphical representation of the function CDH, $TCPA'$and $DCPA'$ is depicted from Figure 6.5.

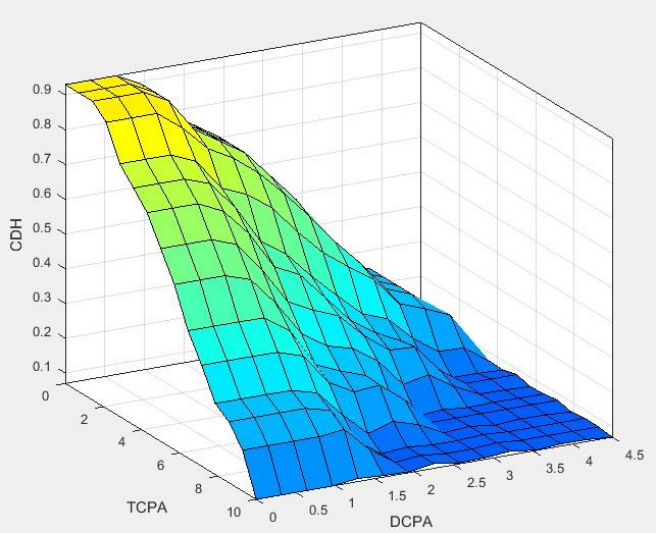

Figure 6.5 Fuzzy Control Surface

The guidance algorithm is expected to perform specific types of manoeuvre, depending on the magnitude of the distance of the waypoint. Some of the important points of the algorithm are described as follows

1. The algorithm doesn't ensure the reachability of waypoints rather reaching the target is the main concern.
2. This algorithm targets two waypoints at a time and chooses an optimal path between two.
3. When the distance to the waypoint is larger it targets to steer towards the waypoint.
4. When the distance to the waypoint is smaller it starts targeting to the next set of waypoints.
5. Nearly zero distance to waypoint makes only small course corrections.

7. CONTROLLER DESIGN

This chapter investigates the control layout of autonomous navigation for the waypoint guidance of WAM-V. The main control law aims to maintain the heading and position to the prescribed path with the desired speed.

7.1 INTRODUCTION

Automatic navigation of the ship is one of the most complicated problems. Usually, highly expert and robust controller is required to make a suitable decision considering various environmental conditions. In this context, the accurate determination of the current position is very important and this problem has been solved by global positioning system (GPS), Inertial Navigation System (INS), Radio Detection and Ranging (RADAR), Magnetic Compass etc. INS and GPS are complimentary navigation systems and can be integrated to produce a more reliable and accurate positioning system (Perera, et al. 2012). Most of the real world applications of the robots are based on accurate positioning and only scale of requirement changes from global navigation to local navigation and personal navigation. Since waypoint tracking is widely used in wheeled mobile robots, surface ships, remotely operated vessels (ROV) and AUV.

There are several control schemes used for autonomous waypoint navigation, namely PID, adaptive and predictive control, sliding mode control, etc. A nonlinear controller for manoeuvring of the underactuated ship was developed (Thor I. Fossen et al. 2003) by utilizing dynamic feedback using backstepping approach. A model free subspace H∞ control for an Atlantis wind propelled catamaran has been developed

(Elkaim et al. 2006). For tracking control of ship manoeuvering a PI-type sliding mode controller was investigated by Ker-Wei Yu et al. (2004). The use of intelligent control in this field became popular in order to achieve better control results. The fuzzy approach was used to study the path following for motion control under disturbances and performance of the controller was compared with the PID (Sanjay et al. 2013).

The guidance problem is to navigate to and cross on a specified heading defined by the series of waypoints. In various marine applications, it is of primary importance to steer the ship along the desired path. The desired path consists of a turning and straight line segments, which is defined by the waypoints. A vessel cannot change its yaw rate instantaneously. There are three phases exist for a turning manoeuvre: zero yaw rate, accelerating/ de-accelerating yaw rate and constant yaw rate (Pandey and Hasegawa 2017). Figure 7.1 shows the guidance problem where the vessel needs to navigate to and cross on a specified heading, to follow a series of waypoints.

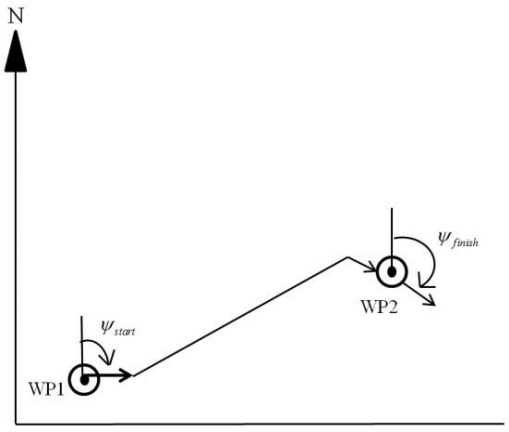

Figure 7.1 The ship departs waypoint1 on a heading ψ_{Start} and is to cross waypoint2 heading ψ_{Finish}. The dots represent the positions of the waypoint.

In general, motion control systems are constructed as three interacting systems. These three systems are the guidance, navigation and control systems. The guidance system provides a reference model with a calculated desired heading, the navigation

system acquires position and attitude of the vehicle, while the control system allocates thrust to the actuators to ensure that desired position and velocity are satisfied. The guidance system keeps track of the desired heading angle that the object shall follow. The desired reference is continuously computed based on the current position given by the navigation system and a target defined by the guidance algorithm. In this chapter, the guidance, navigation and control (GNC) architecture are introduced for the waypoint guidance of WAM-V. The desired heading is fed to the control system so that the autopilot can follow the calculated result.

The GNC architecture is shown in figure 7.2.

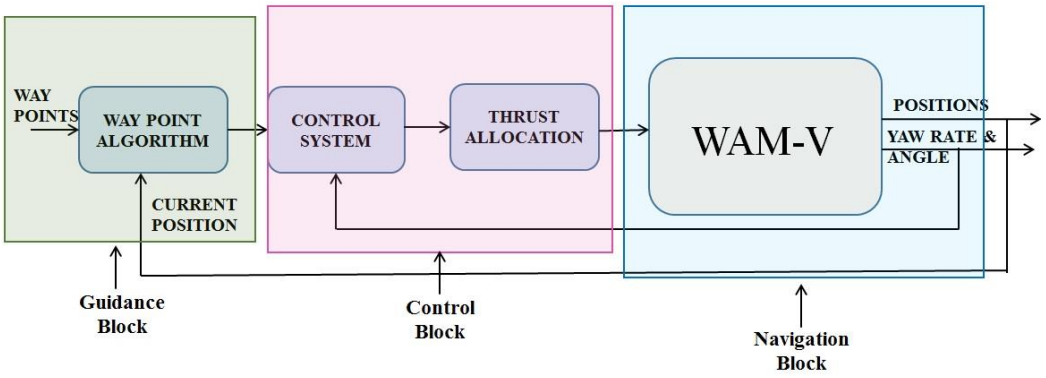

Figure 7.2 Guidance, Navigation and Control architecture

In this research, the fuzzy guided waypoint algorithm is used as a guidance system. After deciding the appropriate course to the waypoint by fuzzy reasoning, PID controller is used to correct the course as a control system.

7.2 CONTROL SYSTEM LAYOUT

Control system layout designed contains two loops as shown in figure 7.3 For outer loop fuzzy controller is used to feed the desired heading to the inner loop. In the inner loop, a PID feedback controller is used to correct the desired course generated by

the fuzzy reasoned algorithm. The control system provides the necessary feedback signal to track the desired heading comes from the fuzzy algorithm. After PID generates the appropriate command, thrusts are allocated to the port side and starboard side thrusters. Finally, thrusts are allocated to both thrusters based on the lookup table which is obtained from the free running model experiments. The thrust allocation problem is briefly discussed in the Chapter 8.

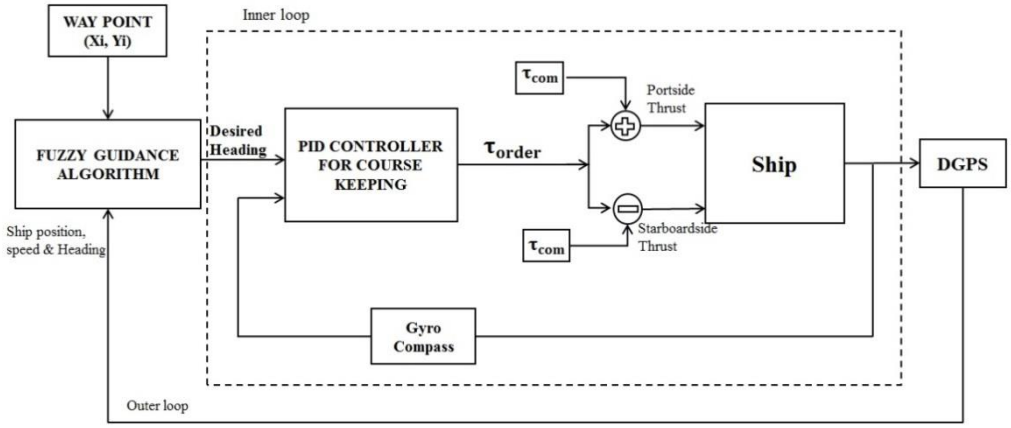

Figure 7.3 Control System Layout

In this control system, waypoints are input in the form of GPS locations. The PID control system provides the necessary feedback signal to track the desired heading comes from the guidance algorithm. Equation (7.1) shows governing equation of PID controller. Where ψ_1 is desired heading calculated with the help of fuzzy reasoning. ψ and $\dot{\psi}$ are the vessel's current heading and yaw rate correspondingly. Where a proportional gain (K_p), Integral gain (K_i) and derivative gain (K_d) are the control design parameters. These parameters are tuned in order to avoid the overshoot and steady state errors and rise time.

$$\tau_{order} = K_p(\psi_1 - \psi) - K_d(\dot{\psi}_1 - \dot{\psi}) + K_i\int_0^t(\psi_1 - \psi) \tag{7.1}$$

Using this proposed controller, simulation is performed in order to check the feasibility of the algorithm, before conducting the pond experiments. In order to tune the PID parameters, some simulations are also performed with the help of the 2nd order Nomoto's model, which is derived from the MMG type of model as discussed in chapter 3. The details of both the simulations are discussed in the following section.

7.3 SIMULATION RESULTS

To verify the effectiveness of the fuzzy waypoint guidance algorithm, the PID feedback control system is simulated with Matlab/Simulink. In this simulation MMG type of mathematical model of WAM-V is used as a system model. Figure 7.4 shows the waypoint guidance and control model in Simulink. The waypoint coordinates are input as Earth-fixed coordinate system. Figure 7.5 shows the reference and the actual trajectory of simulation results. The dotted line indicates the reference trajectory and solid line indicates the actual obtained trajectory. The waypoints are given in latitude and longitude on earth fixed coordinate system as waypoint1= (10, 5), waypoint2= (35, 20) and waypoint3= (50, 16). Here, fuzzy reasons the desired heading and PID generate the control heading, Once PID generate the control output, thrust is allocated with the help of lookup table (Chapter 8) The resulting trajectory seems quite satisfactory. The reference and actual heading graph are plotted in Fig. 7.6. The solid line shows the reference heading and the dotted line shows the heading obtained from the controller. The result is quite satisfactory and proving that the fuzzy guided waypoint algorithm with PID autopilot has a good property of course keeping and changing.

The time history of $TCPA'$ and $DCPA'$ graph is shown in Fig. 7.7 and 7.8. The value of $TCPA'$ is decreasing as the WAM-V is reaching the waypoint. As the

WAM-V reached the waypoint the value became zero, which means after this WAM-V starts targeting the next set of waypoints. The $DCPA'$ graph shows the time history of the distance to reach the waypoint.

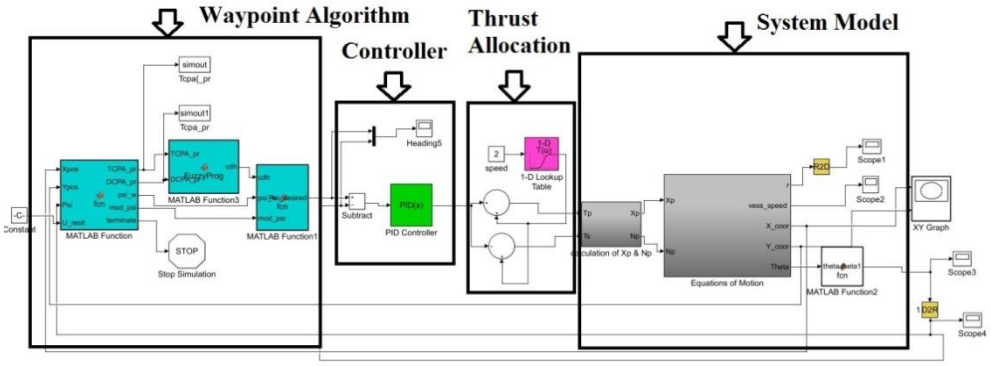

Figure 7.4 Simulink Model for waypoint guidance and control of WAM-V

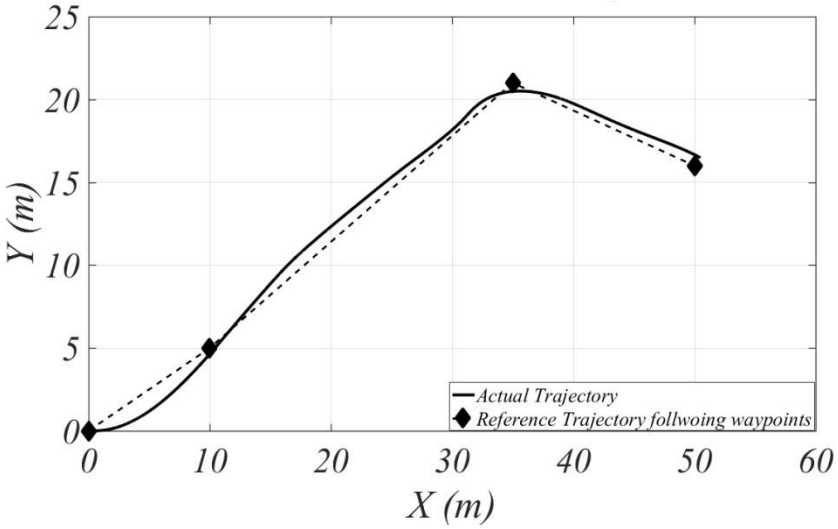

Figure 7.5 Simulated trajectory of WAM-V navigated through the waypoints

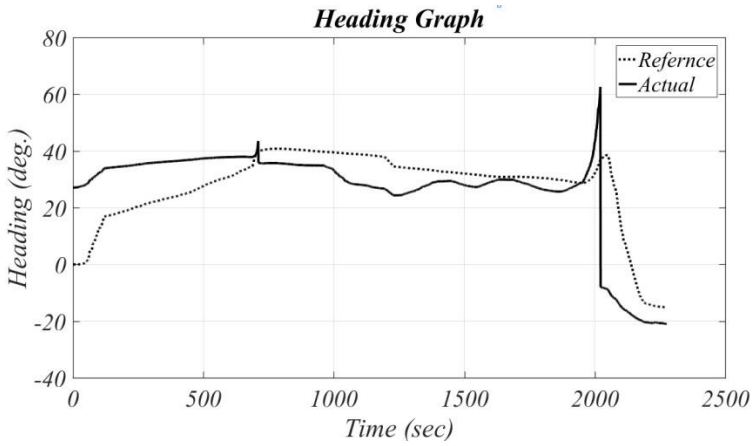

Figure 7.6 References and Actual Heading Graph

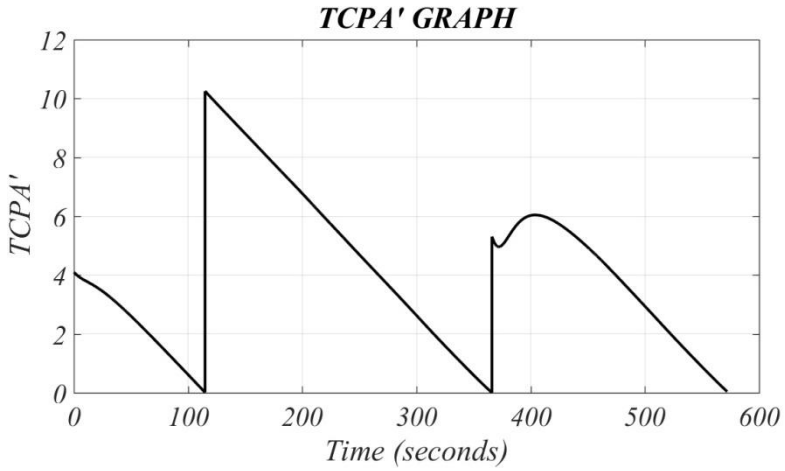

Figure 7.7 Time history of $TCPA'$

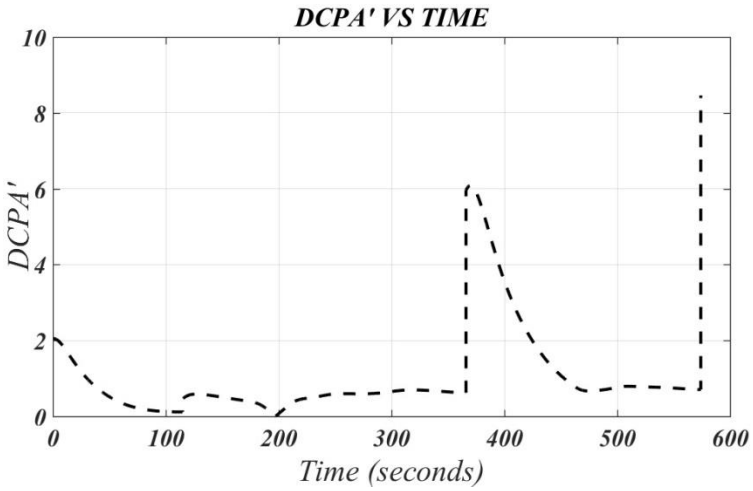

Figure 7.8 Time history of $DCPA'$

In order to tune the PID parameters, the 2nd order Nomoto model derived from the MMG model as discussed in chapter 3 is used in this simulation. 2nd order mass spring damper system is considered as a reference system, which helps to tune the control parameters. The control system provides the necessary feedback signal to track the desired heading angle ψ_d. The output is the yaw moment $(n_{(p)} - n_{(s)})$ and heading angles ψ_d. Figure 7.9 shows the Simulink model of the control algorithm with a Nomoto's model as a plant.

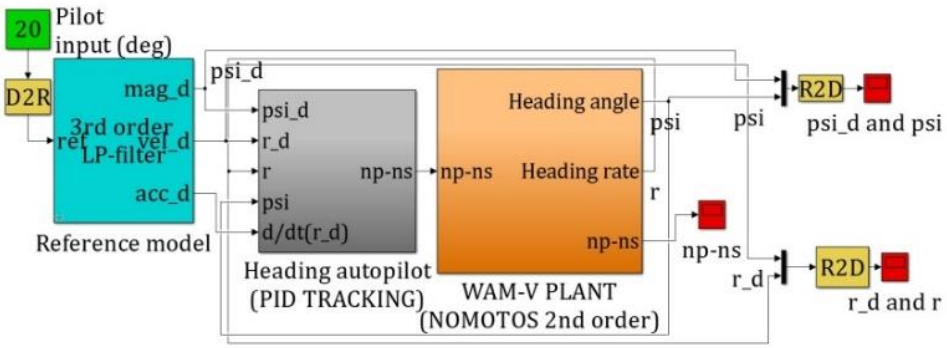

Figure 7.9 PID heading autopilot using Nomoto's 2nd order WAM-V model in Simulink

Without proper tuning of proportional gain (K_p), Integral gain (K_i) and derivative gain (K_d), there is an overshoot as shown in time history as shown in Fig. 7.10 (a) and after tuning K_p =0.18, K_i =0.001 and K_d =0.33 and the time history is shown in Fig. 7.10 (b). These tuned parameters are used for both in simulation and experiments.

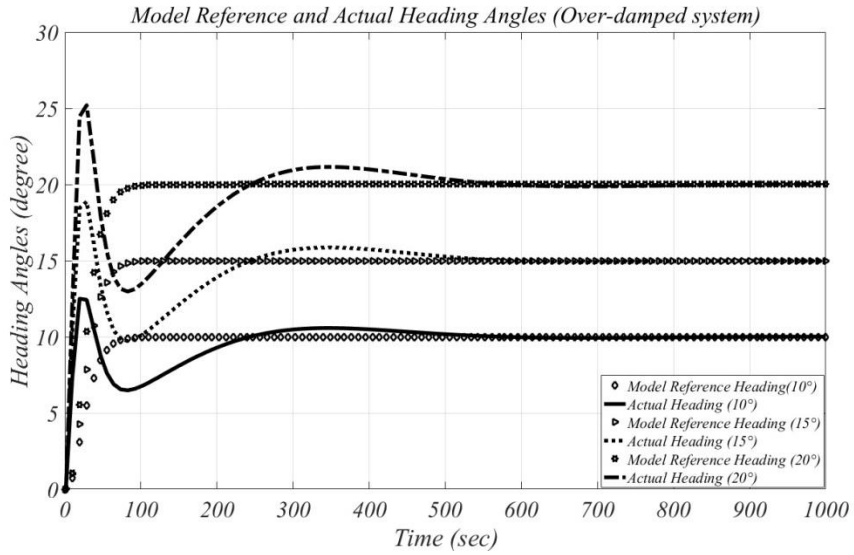

(a)

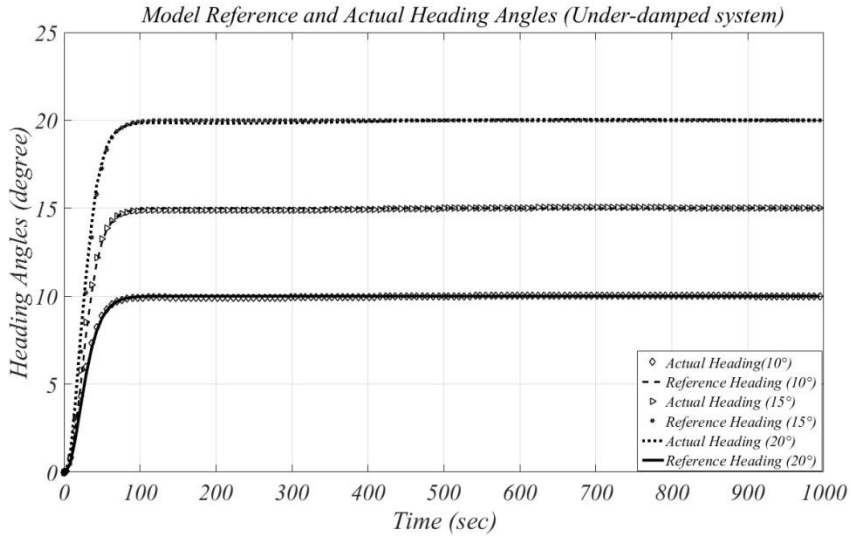

(b)

Figure 7.10 Time history of Heading angles changing with time (a). Without tuning system parameters (b). After tuning system parameters

8. THRUST ALLOCATION

In this chapter, thrust allocation problem for underactuated WAM-V is discussed with the solution. The thrust allocation is a problem of determining desired force supplied to each thruster in order to control the motion of WAM-V.

8.1 BACKGROUND

Thrust allocation is a difficult problem for underactuated and overactuated systems. The underactuated system is a system in which there is a less actuator than needed to satisfy the control objectives. Allocation of the desired thrust using the command information from the controller is challenging due to maintaining both the heading and speed. In marine vehicle, the thrust allocation is represented by equation (8.1)

$$u = K^{-1}T^{-1}\tau \tag{8.1}$$

Where u represents a vector of control input. K diagonal matrix of force coefficient. T is generally non-square thruster configuration matrix and τ is the vector of control forces and moments.

The problem of control allocation for ships and underwater systems are briefly described in the literature. Generally, over actuated system is chosen as it improves the safety of control system in case of actuator fails (Fossen and Johansen 2006) but the same time underactuated system are preferred in order to reduce the cost, maintenance and easily controllability. The catamaran ASV developed for bathymetry survey and environment monitoring in a riverine area also has differential thrust allocation (Hong & Arshad 2015). The Springer ASV (Naeem W. et al. 2007) is also a catamaran vessel

with two inputs. The control allocation is done using common mode and differential mode thrust approach. The design and implementation of a model-based control and control allocation system for WAM-V are discussed (Anderson, 2014) in the literature.

8.2 DISCUSSION

The WAM-V is controlled by differential thrust for the surge, sway and yaw motion control. The desired heading can be generated by differential thrust combinations. The WAM-V can be modelled as two inputs (T_P & T_S) and single output system as shown in Figure 8.1

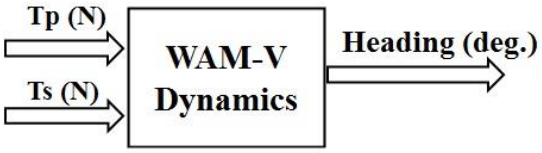

Figure 8.1 Block diagram representation of two inputs WAM-V

The T_P and T_S are the two thrust input supplied to the port side and starboard side. When there is a difference in thrusts between port and starboard sides, three conditions can be generated as described in Equation (8.2), (8.3) and (8.4).

$$(T_P \sim T_S) = 0 \quad \text{Straight Line} \tag{8.2}$$

$$(T_P \sim T_S) > 0 \quad \text{Starboard side Turning} \tag{8.3}$$

$$(T_P \sim T_S) < 0 \quad \text{Port side Turning} \tag{8.4}$$

The final thrust allocation command supplied to the port side and starboard side thrusters could be decomposed into Equation (8.5) and (8.6). τ_{com} represents the common mode thrust and τ_{order} is differential mode thrust coming as a PID output. In order to maintain the speed of the vessel, τ_{com} is generated from a lookup table (Figure

7.3). The differential mode thrust varies depending on the direction of manoeuver.

$$T_{port} = \tau_{com} + \tau_{order} \tag{8.5}$$

$$T_{starboard} = \tau_{com} - \tau_{order} \tag{8.6}$$

In the turning test experiment as discussed in chapter 4, several combinations of differential thrusts cases are studied. During the experiment, the GPS data was stored and analyzed offline to see the turning response of the WAM-V, with the change in the thrust of port and starboard thruster. At various differentials thrust cases of turning circle tests, the input supplied (T_P and T_S) yaw rate and vessel speed data are collected. This data is plotted in the form of a surface plot graph. These graphs show the functional relationship between a designated dependent variable. Figure 8.2 shows the schematic data table layout obtained from the free running experiment test. The given input data notations are same as tabulated in Table 4.2. The figure 8.3 (a) & (b) show surface plot between the corresponding yaw rate and vessel velocity to the port side (T_P) and starboard side (T_S) thrust. These plots show the potential relationship between T_P, T_S, vessel speed and yaw rate.

Given Input	Tp	Ts	Yaw Rate	Vessel Speed
AA	0	0	0	0
BB	2.3	2.3	0	0.2456
CC	10.25	10.25	0	1.09430605
DD	18.56	18.56	0	1.98
EE	21.15	21.15	0	2.25
FF	32.5	32.5	0	3.468
bb	-2.3	-2.3	0	0.24
cc	-10.25	-10.25	0	1.09430605
dd	-18.56	-18.56	0	1.98
ee	-21.15	-21.15	0	2.25
ff	-32.5	-32.5	0	3.468
AB	0	2.3	-0.113	0.124
AC	0	10.25	-0.342	0.53
AD	0	18.56	-0.489	0.904
AE	0	21.15	-0.52	1.01
AF	0	32.5	-0.615	1.44
BC	2.3	10.25	-0.382	0.64
BD	2.3	18.56	-0.514	1
BE	2.3	21.15	-0.5423	1.1
BF	2.3	32.5	-0.63	1.53

Figure 8.2 Schematic picture of lookup table from free running tests

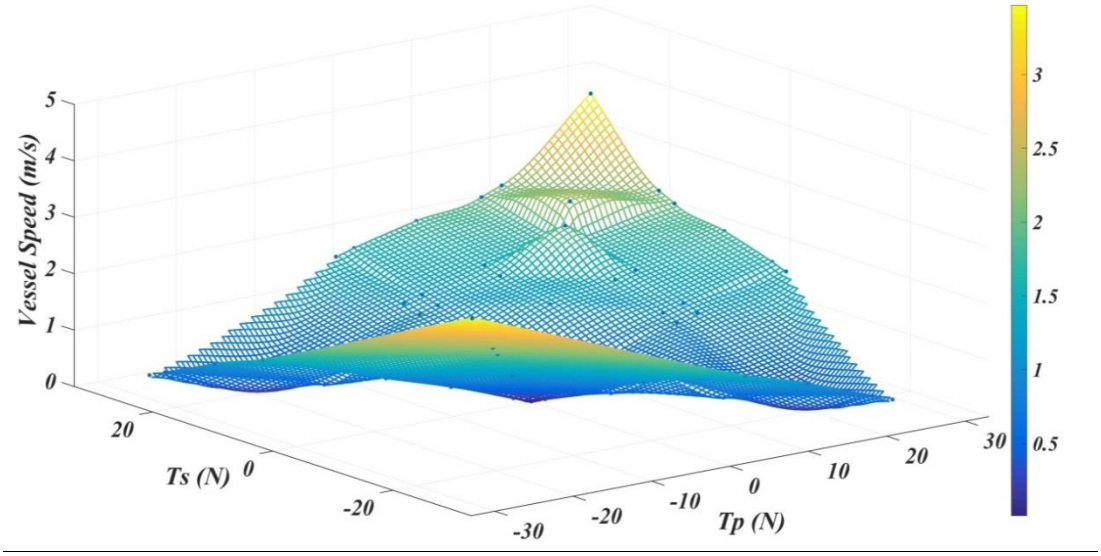

(a)

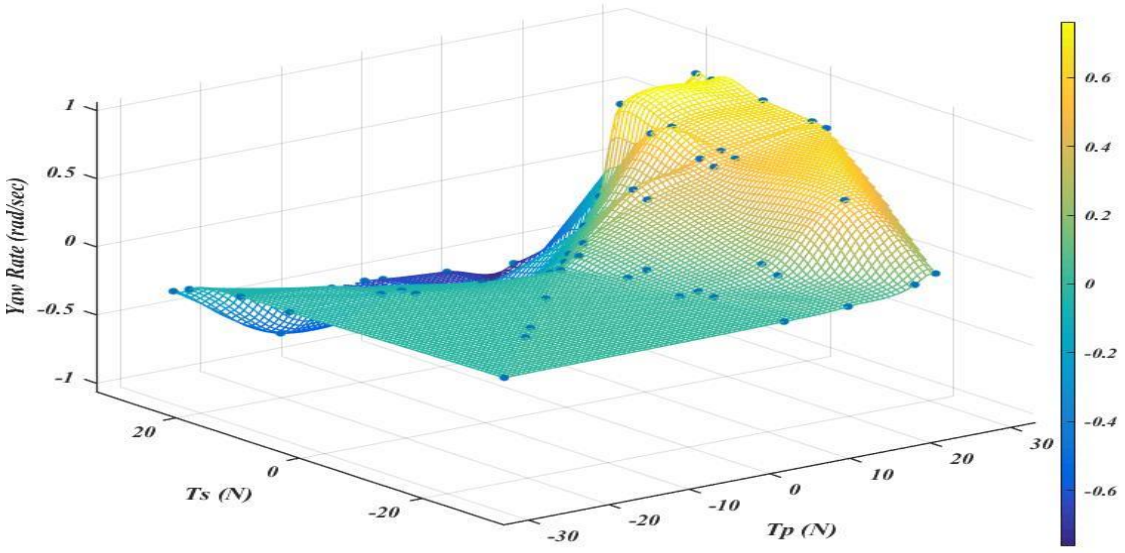

(b)

Figure 8.3(a) surface plot between vessel speed & Tp, Ts (b) surface plot between yaw rate & Tp, Ts

(b)

9. POND EXPERIMENT RESULTS

This chapter presents the experimental results of the waypoint guidance, navigation and control algorithm. Using the proposed waypoint guidance controller in chapter 7, several experiments were conducted at the Osaka University pond facility to validate the robustness and efficiency of autonomously navigated WAM-V through the waypoints. The experimental configuration of WAM-V used for the above mentioned experiment has been delineated in chapter 2. To begin with the experiment, initially random waypoints belonging within the domain of the latitudinal and longitudinal boundary of the pond were selected. During the waypoint selection process, the physical navigational constraint of the WAM-V was always taken care of. Table 9.1 delineates the set of waypoint selected to demonstrate and validate the robustness of the proposed waypoint algorithm. The set of the waypoint given in table 9.1 has been converted to Cartesian coordinated, where the origin, i.e. (0,0) coordinate represented the launching point

Table 9.1 Experimental set of waypoints

Description	Waypoints (x, y)		
	I	II	III
Figure 9.1	21.0,-16.5	-	-
Figure 9.2	5.8,-11.8	6.0,-13.9	-
Figure 9.3	2.7, -1.2	7.8, -3.4	11.9, -8.7
Figure 9.4	10.2, -1.0	22.0, -6.7	34.5, -5.5

As shown in Table 9.1 above four sets of waypoints were selected to prove the

robustness of the waypoint guidance algorithm. The results of each four different kinds of experiments are briefly discussed in the next section. To maintain the uniformity of the experimental results same steps were followed with each set of experiments. Hence, each section dealing with the individual experimental results shows the time history of WAM-V trajectory (i.e. Time history of GPS data), time history of the port side and starboard side thrust calculated by the controller, time history of $TCPA'$, $DCPA'$, CDH and finally the time history of heading error.

9.1 FIRST EXPERIMENT

To begin with, one waypoint was selected (almost belonging to a straight line) to check the feasibility and the response of the designed controller for WAM-V. Figure 9.1 (a) shows the google map view of the experimental pond facility at Osaka University with the first set of the waypoint data set. Figure 9.1 (b) shows the x-y plot of the controlled trajectory followed by the WAM-V in order to navigate through the selected waypoint. From the time history of the trajectory, it can be concluded that the controller and the proposed way point algorithm are robust enough to guide the WAM-V through the desired set of waypoint. Figure 9.1 (c) shows the time history of the allocated thrust. From the time history graph of the allocated thrust, it can be clearly seen that the controller was successful in guiding the WAM-V in a straight line and as the external disturbances such as wind try to deviate WAM-V from the controlled path the controller acts instantly to bring back WAM-V to zero error path. The same has been reflected in Figure 9.1 (d) which shows the time history of $TCPA'$,$DCPA'$, CDH and the time history of heading error graph.

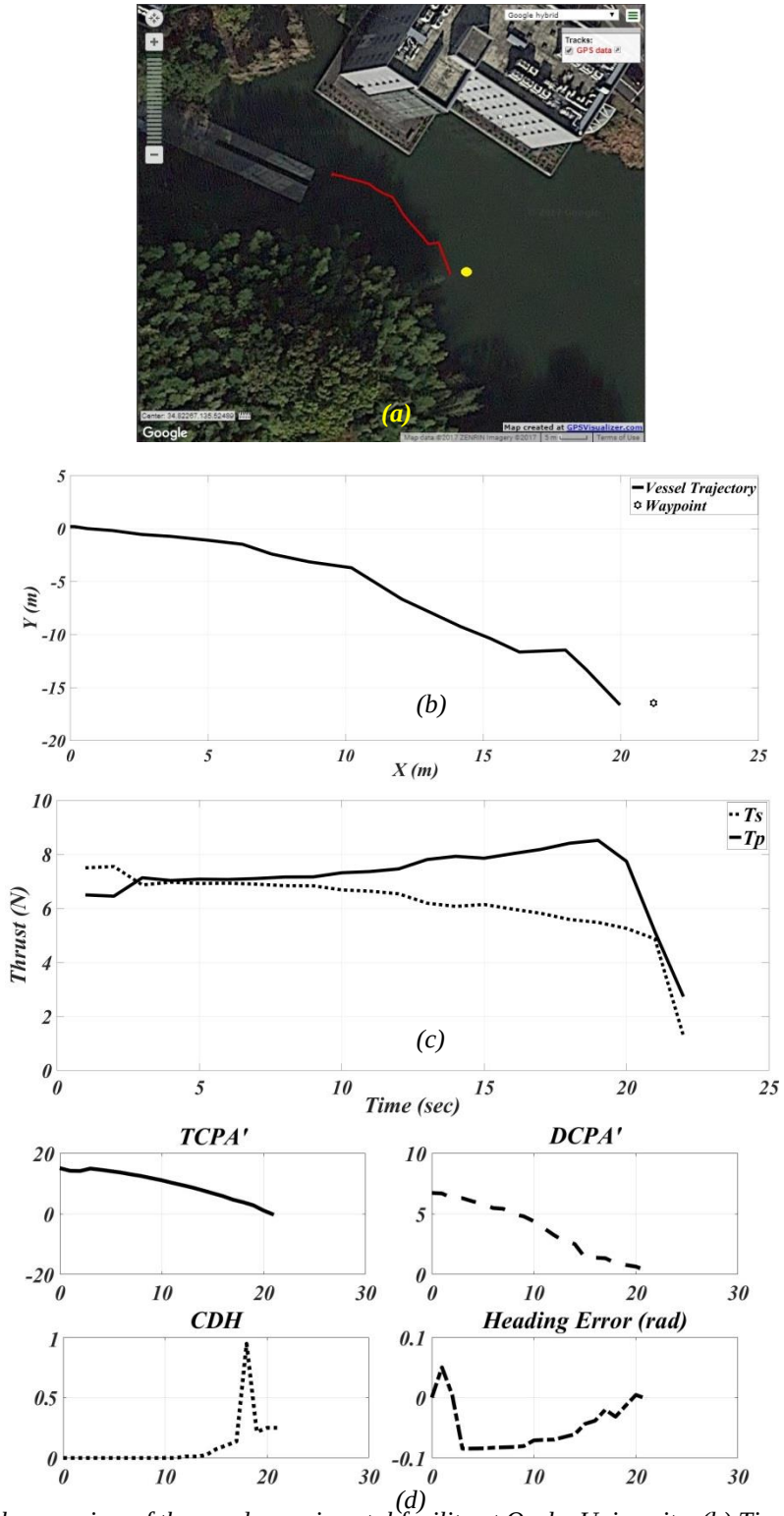

Figure 9.1(a) Google map view of the pond experimental facility at Osaka University, (b) Time history of the controlled trajectory, (c) Time history of the allocated port side and starboard side thrust.(d) Time history of TCPA', DCPA', CDH & Heading Error

From the time history of $TCPA'$ it can be clearly pointed out that the time to the closest waypoint (i.e. $TCPA'$) is reducing as the WAM-V is reaching closer to the waypoint. The distance to the closest waypoint $(DCPA')$ also reduces gradually due to the nearness of the waypoint. In this algorithm, switching of the waypoint is done when the $TCPA'$become negative. WAM-V is stopped near the waypoint because there is no further waypoint assigned in this case. Similarly, CDH (i.e. The parameter deciding which waypoint to follow) is the fuzzy controller output was zero initially until the WAM-V reaching closer to the waypoint CDH changes from 0 to 1. The change in CDH i.e 0 to 1 makes the second waypoint as a reference which is absent in this case so WAM-V stopped near the waypoint. The heading error remains slightly negative and then tends to zero.

9.2 SECOND EXPERIMENT

Figure 9.2 shows the second experimental result, where two waypoints are chosen. Figure 9.2 (a) shows the google map view of the experimental pond facility at Osaka University with the second set of the waypoint. Figure 9.2 (b) shows the x-y plot of the controlled trajectory followed by the WAM-V in order to navigate through the selected set of waypoints. Figure 9.2 (c) shows the time history of the allocated thrust. The thrust is allocated to both the sides of the thrusters according to the desired heading. Port side thrust (Tp) is higher that starboard side due to the turning direction. From the time history graph of the allocated thrust it can be clearly seen that the controller was successful in guiding the WAM-V in a desired turning direction. In Figure 9.2 (d) time history of heading error graph, $TCPA', DCPA'$ and CDH is shown.

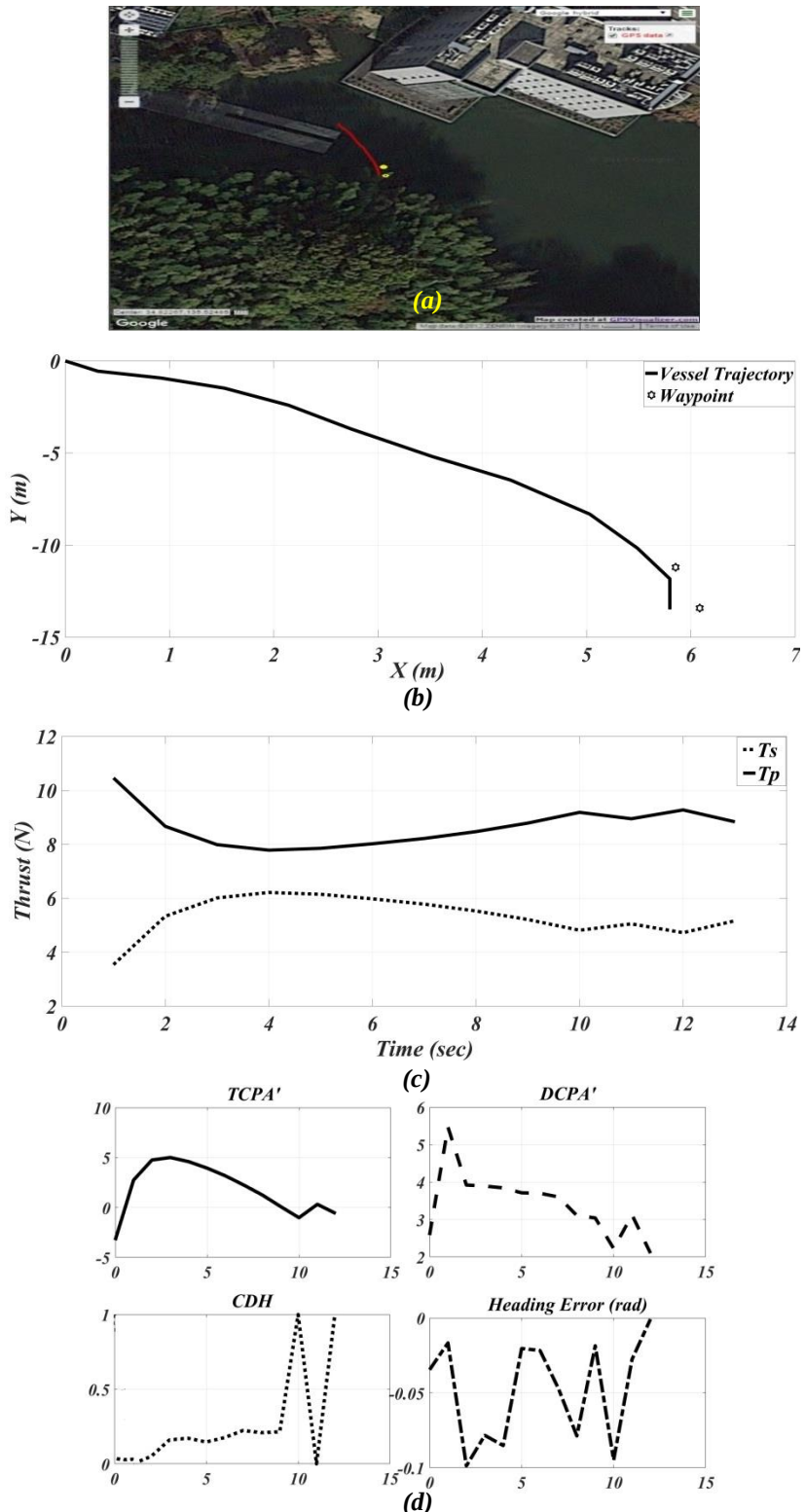

Figure 9.2 (a) Google map view of the pond experimental facility at Osaka University, (b) Time history of the controlled trajectory, (c) Time history of the allocated port side and starboard side thrust. d) Time history of TCPA', DCPA', CDH & Heading Error

The time history of $TCPA'$ plot shows when the WAM-V is reaching to the waypoints it is gradually decreasing and tending towards zero. The value of $TCPA'$ again increased when the WAM-V is started targeting to the second waypoint. The second waypoint is closer to first do it doesn't increase much. The $DCPA'$ plot shows the distance approaching towards the waypoint, which is decreasing with time and again increase due to next waypoint. The value of CDH is calculated with the fuzzy reasoning which gradually increased due to the nearness of the waypoint and again decreased. The heading error is also within the range. This test demonstrates the action taken by the vessel in order to reach the waypoint. This experiment proves the effectiveness of the waypoint algorithm.

9.3 THIRD EXPERIMENT

For the third test, 3 waypoints are chosen. Figure 9.3 (a) shows the google map view of the experimental pond facility at Osaka University with the third set of the waypoint data. Figure 9.3 (b) shows the x-y plot of the controlled trajectory followed by the WAM-V in order to navigate through the selected set of waypoints. From the time history of the trajectory it can be concluded that the controller and the proposed way point algorithm are robust enough to guide the WAM-V through the desired set of waypoint.

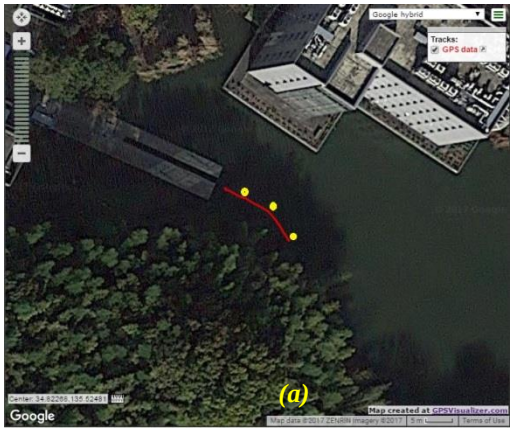
Google hybrid
Tracks:
GPS data
(a)
Google
Map created at GPSVisualizer.com

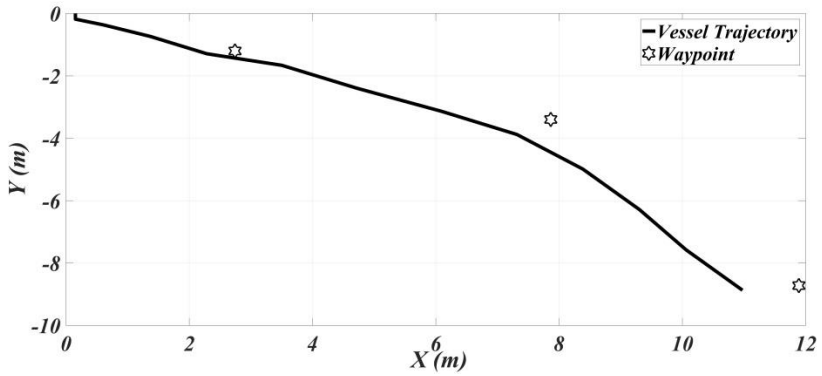
Vessel Trajectory
Waypoint
Y (m)
X (m)
0
-2
-4
-6
-8
-10
0
2
4
6
8
10
12

(b)

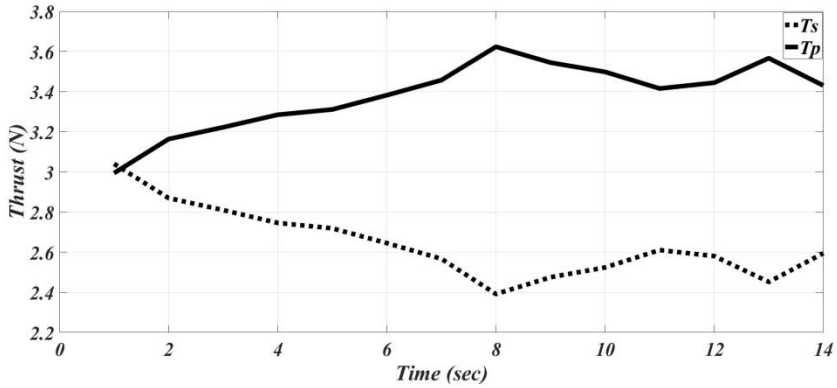
Ts
Tp
Thrust (N)
Time (sec)
3.8
3.6
3.4
3.2
3
2.8
2.6
2.4
2.2
0
2
4
6
8
10
12
14

(c)

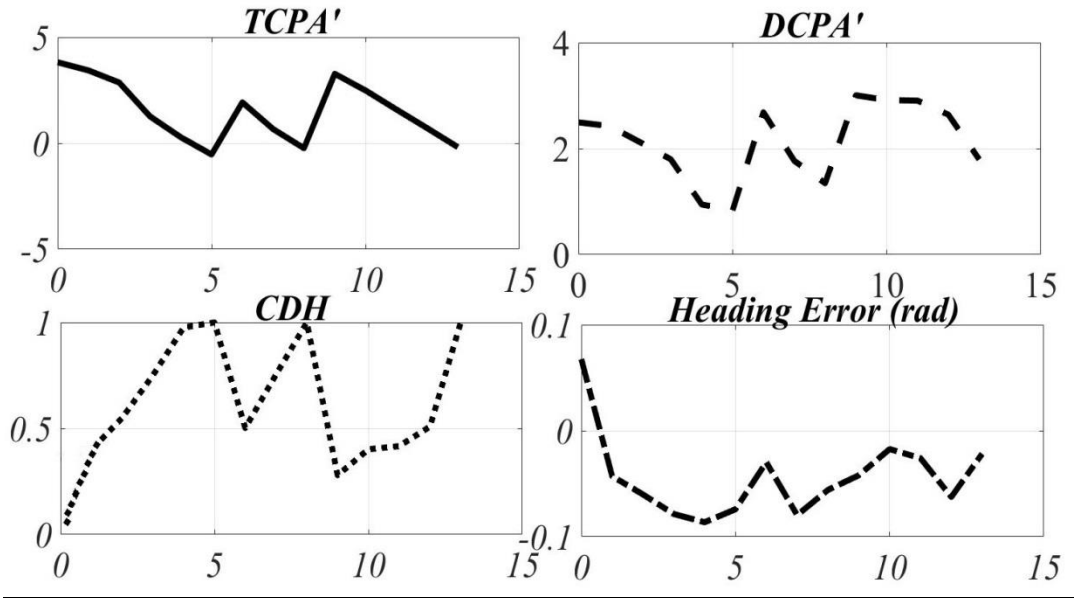

(d)

Figure 9.3 (a) Google map view of the pond experimental facility at Osaka University, (b) Time history of the controlled trajectory, (c) Time history of the allocated port side and starboard side thrust. d) Time history of $TCPA'$, $DCPA'$, CDH & Heading Error

Figure 9.3 (c) shows the time history of the allocated thrust. From the time history graph of the allocated thrust, it can be clearly seen that the controller was successful in guiding the WAM-V in a turning direction. The behaviour shows that the T_P is higher than T_S in order to follow the desired course. The same has been reflected in Figure 9.3 (d) which shows the time history of $TCPA'$,$DCPA'$, CDH heading error graph. $TCPA'$ become negative three times, which shows the reachability of every waypoint. $DCPA'$ shows the distance of the waypoint from the vessel at each waypoint. CDH is calculated according to the fuzzy rules defined and shows the degree of closeness to the waypoint. The heading error remained slightly negative and gradually tends to zero.

9.4 FOURTH EXPERIMENT

Figure 9.4 shows the result of the 4th set of waypoints, where 3 waypoints are chosen in a zigzag manner. Figure 9.4 (a) shows the google map view of the experimental pond facility at Osaka University with the fourth set of the waypoint data set. Figure 9.4 (b) shows the x-y plot of the controlled trajectory followed by the WAM-V in order to navigate through the selected set of waypoints. The vessel trajectory shows good agreement in terms of the reachability of the waypoint. Figure 9.4 (c) shows the time history of the allocated thrust. The thrust graph shows the variation of the thrust between port side and starboard side, according to the reference course. From the time history graph of the allocated thrust it can be clearly seen that the controller was successful in guiding the WAM-V in a zigzag pattern and as the external disturbances such as wind tries to deviate WAM-V from the controlled path the controller acts instantly to bring back WAM-V to zero error path. The same has been reflected in Figure 9.4 (d) which shows the time history of of $TCPA'$, $DCPA'$,CDH and heading error graph.

The $TCPA'$ plot became negative whenever the waypoint passed and shows the switching to the next waypoint. The $DCPA'$ plot shows the time history of the distance covered in order to chase each waypoint. The value of CDH is calculated with the fuzzy reasoning. The heading error is also within the acceptable range of limit. This algorithm is not very accurate in terms of the reachability of waypoint but it is very robust for navigational path planning. In some of the real applications, it is not necessary to reach the waypoint but to navigate through the points are very important and this algorithm is very feasible in such cases.

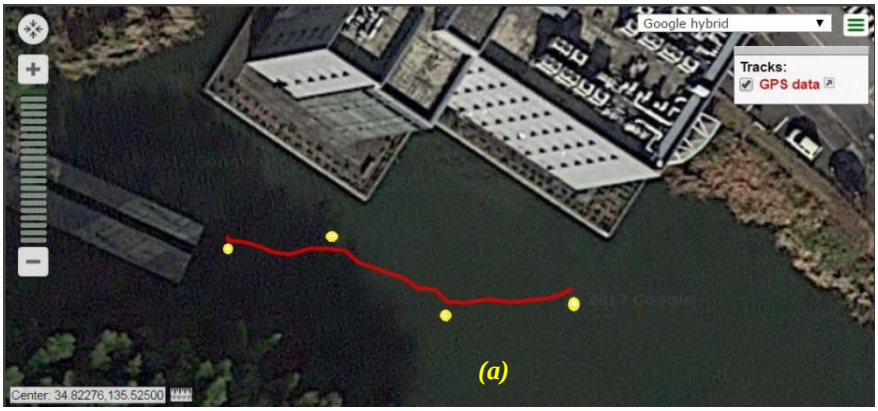
Google hybrid
Tracks:
GPS data
Center: 34.82276,135.52500

(a)

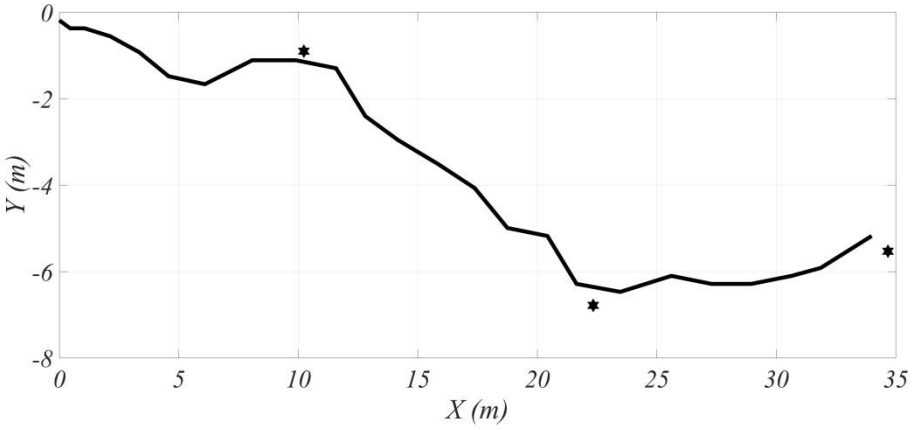
0
-2
-4
-6
-8
Y (m)
0
5
10
15
20
25
30
35
X (m)

(b)

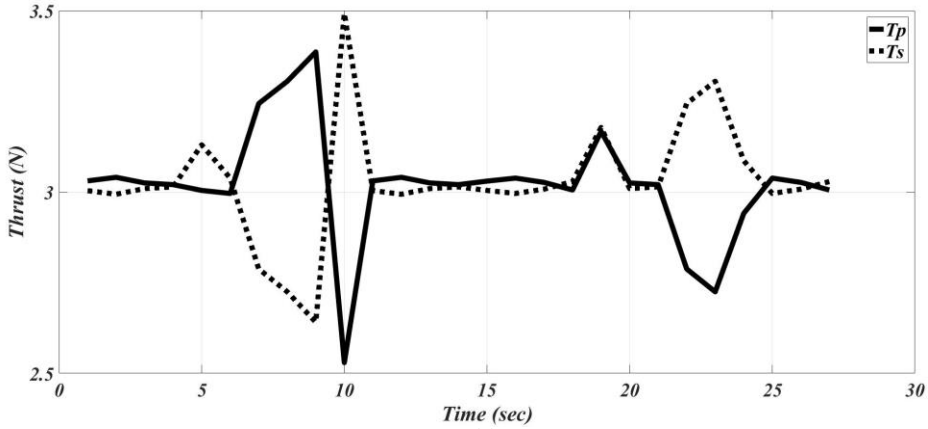
3.5
3
2.5
Thrust (N)
0
5
10
15
20
25
30
Time (sec)
Tp
Ts

(c)

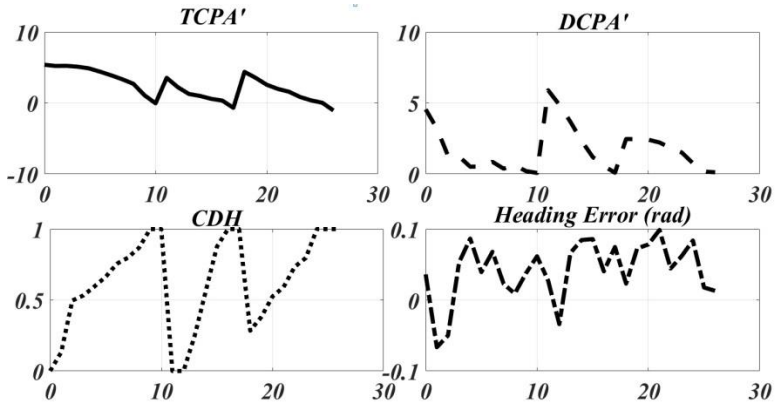

(d)

Figure 9.4 (a) Google map view of the pond experimental facility at Osaka University, (b) Time history of the controlled trajectory, (c) Time history of the allocated port side and starboard side thrust. d) Time history of $TCPA'$, $DCPA'$, CDH *& Heading Error*

10. CONCLUSION AND FUTURE WORK

10.1 CONCLUSION

In this research, catamaran WAM-V is introduced with its navigational and control performance.

The first task was to develop WAM-V with integrating all sensors and electronics to make it capable of recording actuator input commands and sensor data, which is successfully accomplished. It is observed that the WAM-V software and hardware module is sufficient to be used for navigation and control research which is described in Chapter 2.

In Chapter 3, to predict the hydrodynamic behaviour of the WAM-V, an MMG type of mathematical model is investigated. The MMG model has been found suitable to model twin hull- twin propeller system like WAM-V. The MMG model has advantages that it models the hull, propeller and their interaction force separately so even if there is insufficient modelling in one part it is not required to change the full mathematical model. Motion equations for turnable propellers are also derived using MMG-type of model. The second order Nomoto's model was derived from MMG model which integrates the effect of propeller and rudder of conventional ships. The difference between a traditional ship motion response equation and WAM-V motion response equation is that the manoeuvre control variable is generated by the force caused by the thrust difference between port and starboard side thrusters.

In chapter 4, the study of manoeuvring behaviour using captive model tests and free running tests is discussed. The manoeuvring behaviour of the WAM-V is needed to understand well in order to design a controller for autonomous navigation. The motion

of the WAM-V is affected by hydrodynamics, so it was primarily important to estimate manoeuvring derivatives of WAM-V. The two types of captive model tests were conducted at Osaka University towing tank facility. At first resistance test was conducted for mono hull and full catamaran in order to study the hull interference effect on the total resistance of a WAM-V advancing in calm water. It was observed from the resistance test, that at higher velocity (Fn > 0.3), total resistance force on the full catamaran ship is lower than the twice of one hull. The difference in resistance is less marked in the low Froud number (Fn < 0.3). Some of the manoeuvring derivatives such as $Y_v, Y_{vvv}, N_v, N_{vvv}$ are calculated with the help of drift tests, which are used as the initial guesses for system identification method. Because of the lack of RAT facility, some of the manoeuvring derivatives remained unknown, which is calculated with the help of system identification method. To validate the MMG mathematical model and to judge the predictability during course changing, turning simulation with different thrust combination is compared with free running experimental results for both port and starboard side turning. The speed test is conducted in order to understand the relation between the speed of WAM-V and voltage supply to the propellers. Turning ability of WAM-V was studied and two cases were investigated. In the first case, the sense of rotation of both the propellers was different and in the second case, the sense of rotation of both the propellers was same while supplying different thrust combinations to port and starboard side propellers. In order to better quantify the vehicle dynamics with respect to autonomous control, free running model test has enabled significant advances made in the understanding of high speed vehicles The free running input-output data was also used for identifying some of the manoeuvring derivatives of MMG model which could not be calculated with Captive model tests.

In chapter 5, While it was not possible to conduct the RAT or CMT in the towing test, the alternative method (system identification) to calculate those parameters is discussed briefly. The system identification technique was used, which can predict or tune the system parameters in the mathematical model of a WAM-V from measured data of free running experiments. Many of these manoeuvring derivatives are very difficult to measure empirically and experimentally. Speed tests and turning circle tests were conducted and sufficient data were collected to use as an input-output in order to perform parameter identification technique. Finally, this chapter concludes the methodology to calculate the unknown hydrodynamic parameters of the MMG type of model with the help of captive model test, free running test and system identification method.

In chapter 6, a robust waypoint algorithm which is reasoned by fuzzy logic is discussed. The linguistic variables ($TCPA', DCPA'$ and CDH), membership functions and fuzzy control rules are discussed briefly. The fuzzy control rules are constructed based on the human operator's experience as defined in the literature. To verify the effectiveness of the fuzzy waypoint guidance algorithm, the feedback PID control system is simulated with the help of Matlab/Simulink. The second order Nomoto's model derived from the motion equation of WAM-V (Chapter 3) along with model reference heading generator was used to tune PID heading controller parameters. The effect of tuned PID parameter and untuned PID parameter on heading response of WAM-V was studied. From the simulation results, PID heading controller with tuned parameters was found effective to use further in control experiments. The waypoint algorithm is comparatively simple and robust, i.e. can be implemented in any kind of system. In many cases, the behaviour and decision making of ship navigators are done

using fuzzy theory. Fuzzy theory is suitable for complicated and hierarchical human behaviours. These kinds of expert system can apply to the more realistic environmental conditions.

In chapter 7, fuzzy guided double loop control layout for waypoint navigation is discussed. The outer loop is fuzzy reasoned and the inner loop is PID controller. The outer loop generates the desired course to the waypoint utilizing fuzzy reasoned algorithm. The PID controller takes necessary action for course correction after getting the desired course from fuzzy reasoned algorithm. Based on the value of the $TCPA'$ and $DCPA'$, the nearness of the next waypoint is judged and the reference degree (CDH) to the second next waypoint is generated. Therefore, based on the nearness of two consecutive waypoints, fuzzy controller gradually modifies the desired course. The double loop fuzzy waypoint controller is very simple, computationally inexpensive and flexible to sudden changes in the desired path.

In chapter 8, the thrust allocation problem for underactuated WAM-V is discussed. The lookup table based method is introduced to allocate the desired thrust. The lookup table is constructed with the help of manoeuvring experiments. With the given yaw rate and vessel speed a unique T_P and T_S can be assigned to the thrusters The lookup table based thrust allocation method has the advantage to control the vessel speed and yaw rate at the same time.

In chapter 9, the pond experimental results of waypoint navigation are discussed. The results of the experiments are quite promising. Several combinations of waypoints are chosen as input to check the feasibility of the proposed controller. There are many application possibilities using this algorithm for path planning.

This research also proves the advantage of underactuated scheme. The control

law has a concise form and easy to implement in the practice due to a smaller computational burden with only a few online parameters being tuned. The use of free running models also provides the opportunity to test in open water conditions, which not only reduces reliance on high cost test facilities but is also of particular importance for high speed crafts.

One of the purposes of this research is to present a solution to the waypoint tracking problem for a class of underactuated catamaran vessels. This could be owned to a design choice. From a practical perspective, designing a controller for the underactuated system is easier. Underactuated provides backup control techniques for a fully actuated system. If a fully actuated system is damaged or failed, then a controller for the fully actuated system is available to recover from the problem.

10.2 FUTURE WORK

Future work towards testing and improving the autonomous behaviour of the WAM-V needs to incorporate more sensors such as camera and LIDAR.

In this thesis, the underactuated control scheme for waypoint navigation is proposed. In the case of actuator failure, fault tolerance based controller is always an emerging key to the safety point of view. Future work incorporates the fault tolerant based controller to ensure safety in automatic control.

11. REFERENCES

Abkowitz, M.A. (1964) *Lectures on ship hydrodynamics – Steering and maneuvrability. Hydro- og Aerodynamisk Laboratorium*, Report No. Hy-5, Lyngby, Denmark

Abkowitz, M.A. (1980) *Measurement of hydrodynamic characteristics from ship maneuvering trails by system identification*. SNAME Transaction, vol. 88, pp. 283-318

Ahmed, Y. A., Hasegawa, K. (2016) *Fuzzy Reasoned Waypoint Controller for Automatic Ship Guidance*, 10th IFAC Conference on Control Applications in Marine Systems CAMS, vol. 49, issue 23, pp 604-609

Alves, J., Oliveira, P., Oliveira, R., Pascoal, A., Rufino, M., Sebastiao, L., Silvestre, C. (2006) *Vehicle and Mission Control of the DELFIM Autonomous Surface Craft*, Control and Automation. MED'06, 14th Mediterranean conference, Ancona

Amerongen, JV, Naute Lenke, HR, and Veen der Van, JCT, (1977) *An autopilot for ships designed by with fuzzy sets*. Proc. IFAC Conference on Digital Computer Applications to Process Control. The Hague. pp. 479-487

Andrea A. S. (2013) *Simulation of Wave- Adaptive Modular Vessel Suspension system for improved dynamics*, Masters thesis, Virginia Polytechnic Institute and State University

Anderson, M. (2014*). Model-Based Control and Control Allocation System for a WAM-V*, Flinders University, Australia

Ankudinov V., Kaplan P., Jacobsen B.K. (1993) *Assessment and principal structure of the modular mathematical model for ship maneuverability prediction and real-time maneuvering simulations*. Prepared for delivery at MARSIM '93, St. John's, Newfoundland, Canada

AUVSI Foundation, National University of Singapore School of Engineering and Singapore Science Center (2014). Maritime RobotX Challenge Available: http://www.robotx.org/

Beard, R.W. and Maclain T.W. (2012) *Small Unmanned Aircraft Theory and Practice*. Princeton University Press

Broglia, R., Jacob, B., Zaghi, S., Sterm, F. and Olivieri, A. (2014) *Experimental Investigation of Interference effects for high-speed catamarans, Ocean Engineering Journal*, Elsevier, vol. 76, pp 75-85

Caccia, M., Bibuli, M., Bono, R., Bruzzone, G.,. and E. Spirandelli, (2008) *Unmanned Marine Vehicles at CNR-ISSIA*. In proc. of the 17th world congress International Federation of Automatic Control Seol, Korea

Caccia, M., Bruzzone, G. and Bono, R (2008) *A practical Approach to Modeling and Identification of Small Autonomous Surface Craft*, IEEE J. Ocean. Eng., vol. 33, no. 2, pp 133-145

Casson, L. (1964) *Illustrated History of Ships & Boat*s, Doubleday, 1st edition, Oakland, CA

Cheng, J. and Yi, J. (2006) *A new fuzzy Autopilot for way-point tracking control of ships*. IEEE International Conference on Fuzzy Systems, Canada, pp. 451-456

Davidson, K.S.. and Schiff, L.I. (1946) *Turning and Course- Keeping Qualities of ships*. Transactions of SNAME, vol. 54

Driankov, D.,Hellendoorn, H. and Reinfrank, M. (1996) *An introduction to fuzzy control*, Second edn, Springer-Verlag, Berlin

Elkaim, G.H. (2001) *System Identification for precision control of a wingsailed GPS-guided Catamaran*. Ph.D. Thesis, Stanford University, Stanford, CA, December.

Elkaim, G.H. and Kelbley, R.J. (2006) *Control architecture for segmented trajectory following of a wind-propelled autonomous catamaran*. American Institute of Aeronautical and Astronautics, pp 1-14

Elkaim, G.H., Woodley, B.R., and Kelbley, K.J., (2006) *Model Free Supspace H control for an autonomous catamaran*, Position, Location and Navigation Symposium, pp. 1005-1014, IEEE/ION, Coronado

Elkaim, G.H. (2008) *System identification-based control of an unmanned autonomous wind-propelled catamaran*, Control Eng. Practice, vol. 17, pp. 158-169

Faltinsen, O.M., (2005) *Hydrodynamics of High-Speed Marine Vehicles*. Cambridge University Press

Fang, M.C., Luo, J.H., and Lee, M.L. (2005) *A Nonlinear Mathematical Model for ship turning circle simulation in waves*. Journal of Ship Research, vol. 49, No. 2, pp. 69-79

Ferreira, H., Martins, A., Dias, A., Almedia, C., Akmedia J.M., and Silva, E.P. (2006) *Roaz autonomous surface vehicle design and implementation*. Robotica, Portugal, 2006

Fossen T.I. (1994) *Guidance and Control of Ocean Vehicles*, John Wiley & Sons, 1994

Fossen, T.I., Breivik, M. and Skjetne, R. (2003) *Line-of-sight path following of underactuated marine craft*, IFAC Manoeuvring and Control of Marine Craft, vol. 36, issue 21, pp 211-216

Fossen, T.I. and Johansen, T.A. (2006) *A survey of Control Allocation method for Ships and Underwater Vehicles*. MED 06 14th Mediterranean Conference on Control and Automation, Italy

Hajivand, A. and Mousavizadegan, S. H. (2015) *Virtual Simulation of Maneuvring captive model test for a surface vessel*, J. Nav. Archit. Ocean Engineering, vol. 7, pp. 848-872

Hasegawa, K., Kouzuki, A., Muramatsu, T., Komini, H., and Watabe, Y. (1986) *Ship auto-navigation fuzzy expert system (SAFES)*. Journal of society of naval architects of Japan, pp. 445-452

Hasegawa, K. (1990) *Automatic navigator-included simulation for narrow and congested waterways*. Proc. Of ninth ship control systems symposium. 2, pp. 110-134

Hasegawa, K. (1993) *Knowledge-based automatic navigation system for harbour manoeuvring*. Proc. Of tenth ship control system symposium 2. pp. 67-90

Hirano, M. and Takashima, J. (2010) *Ship Maneuverability-Theory and its Applications*. Mitsui Akishima Research laboratory, Japan

Hong, M. J and Arshad, M.R., (2015) *Modelling and Motion Control of a riverine autonomous surface vehicle (ASV) with differential thrust*, Journal Teknology (Science & Engineering) vol. 74, pp. 137-143

Hornaryar, A., Mousavizadegan, S.H., and Ghassemi, H. (2014). *Simulation of Turning Circle Manoeuver of a Catamaran Planning Boat with a Combined Experimental and Numerical Method*. X HSMV- Naples

Im, N.K., and Seo, J.-H. (2010) *Ship Manoeuvring Performance Experiments using a Free Running Model Ship*. Journal of Marine Navigation and Safety of Sea Transportation, vol. 4, pp. 29-33

Inoue, S., Hirano, M., Kijima, K. and Takashima, J. (1981) *A Practical Calculation Method of Ship Maneuvering Motion*. ISP, Vol. 28, No.325

Jia, B. et al. (2012) *Design and Stability Analysis of Fuzzy Switched PID controller for Ship Track Keeping. Journal of Transportation Technologies*, Vol. 2, pp. 334-338

Kempf, G., Foerster U..E. (ed.); *Hydromechanische Probleme des Schiffsantriebs*, Humberg 1932; 2,4,8, 41

Lawless, J., Maurios, M., Roy, J. and Bonafaux, J. (2007), *Design Development and Engineering of the world's largest sailing Catamaran,* RINA- Modern Yacht Conference

Lee, S.M., et al. (2004) *A Fuzzy Logic for Autonomous Navigation of Marine Vehicles Satisfying COLREG Guidelines*. International Journal of Control, Automation, and Systems, Vol. 2, No. 2, pp. 171-181

Ljung, L. (1999) *System Identification: Theory for the user*. Prentice-Hall Inc. 2nd ed., New Jersey

Mamdani E. H. (1974). *Application of fuzzy algorithms for control of a simple dynamic plant*, Proc.

IEEE, 121:1585–1588. [This is the seminar paper on control application of fuzzy theory]

Maneuvering Committee Report (1999), Proceedings of 22nd IITC, Vol. 1

Maneuvering Committee Report (2011), Proceedings of 26th IITC, Vol 1., Rio De Janeiro, Brazil

Manley, J.E. (1997) *Development of the Autonomous Surface Craft "ACES"*. OCEANS'97 MTS/IEEE conference Proceedings Halifax. NS, Volume (2), pp.827-832

Maritime Advanced Research Inc. *Wave Adaptive Multipurpose Vessel*, http://www.wam-v.com/

Moreira, L., and Soares, C.G. (2011) *Autonomous Ship Model to perform Manoeuvring tests. Journal of Marine Research*, vol. VII, no. 2, pp. 29-46

Motora, S. (1959 and 1960). *On the measurement of Added Mass and Added Moment of Inertia for Ship Motions (Part 1,2 and 3)* (In Japanese). Journal of SNAJ, vol. 105 and 106

Mousaviraad, M., Bhushan, S. and Stern, F. (2013) *URANS studies of WAM-V Multi-Body Dynamic in Calm Water and Waves.* 3rd International Conference on Ship Manoeuvering in Shallow and Confined water, At Ghent, Belgium

Naeem, W., Sutton, R. and Chudley, J. (2003) *System Identification, Modelling and Control of an Autonomous Underwater Vehicle*, Proceedings of the MCMC IFAC Conference, Girona, Spain

Naeem, W., Sutton, R. and Chudley, J. (2006) *Modelling and Control of an Unmanned Surface Vehicle for environmental* Monitoring, UKACC International Control Conference, Glasgow, Scotland, UK

Naeem, W., and Xu, T., Sutton, T. and Tiano, A. (2007) *The design of navigation, guidance and control system for an unmanned surface vehicle for environmental monitoring*, J. Engineering for the maritime environment, vol. 222, pp 67-79

Nomoto, K. (1964) *Ship Maneuverability* (in Japanese). Text of the 1st Symposium on the Ship Maneuverability, SNAJ

Nordtvedt, S.A. (1996) *A History of Catamaran Design and Construction in Australia, Society of Naval Architects and Marine Engineers*, Pacific Northwest Division, pp. 1-23.

Ogawa, A., Koyama, T., Kijima, K. (1977) *MMG report on the mathematical model of ship manoeuvring*. Bull Soc Naval Archit Jpn. 575-28 (in Japanese)

Ogawa, A., Kasai, H. (1978) *On the mathematical model of manoeuvring motion of ships*. Int. Shipbuild prog 25 (292); 306-319

Oh, S.R., Sun, J., Li, Z., Celkis, E.A. and Parsons, D. (2010) *System Identification of Model Ship*

using a Mechatronic System, IEEE/ASME Transaction on Mechatronics, vol. 15, no. 2

Oh, S.R. and Sun, J. (2010) *Path Following of underactuated Marine Surface Vessels using line-of-sight based model predictive control*. Ocean Engineering, Elsevier, pp 289-295

Pandey, J., and Hasegawa, K. (2017) *Autonomous Navigation of Catamaran Surface Vessel*, IEEE OES Symposium on Underwater Technology (UT), pp. 1-6, Busan

Peterson, A. W. (2013) *Simulation and testing of Wave Adaptive Modular Vessel*. Doctor of Philosophy, Virginia Polytechnic Institute and state university

Perera, L.P., Moreira, L., Santos, F.P., Ferrari,V., Sutulo, S. and Soeares, C.G., (2012*), A Navigation and control platform for real-time manoeuvring of Autonomous Ship Models*, 9th FAC Conference n Manouvring and Control of Marine Craft (MCMC), Italy, Vol. 5, No. 5, pp. 465-470, Sep. 2012.

Sanjay, A. J. and Hariprasad, S.A. (2013) *Performance Analysis of Ship Tracking using PID/Fuzzy Controller*, Internationa Journal of computer trends and technology (IJCTT), vol. 4, issue 6, pp. 1858- 1861

Stern, F., Agdrup, K., Kim, S. Y., Hochbaum, A. C., Rhee, K. P., Quadvlieg, F., Perdon, P., Hino, T., Broglia, R., and Gorski, J. (2011) *Experience from 2008 — The First Workshop on Verification and Validation of Ship Maneuvering Simulation Methods*, Journal of Ship Research, Vol. 55, No. 2, pp. 135-147

Wirtensohn, S., Reuter, J. Blaich, M., Shuster, M. and Hamburger, O. (2013) *Modelling and Identification of a Twin Hull-Based Autonomous Surface Craft*, IEEE-Methods and Models in Autonomous and Robotics (MMAR), pp 121-126

WAM-V, Wave Adaptive Modular Vessel,. Available: http://www.wam-v.com/wamv.html

Xu, T., Chudley, J. and Sutton, R. (2006) Soft computing design of a multi-sensor data fusion system *for an unmanned surface vehicle navigation*. In proc. of 7th IFAC conference on manoeuvring and control of marine craft

Yasukawa, H., Yoshimura, Y. (2015) *Introduction of MMG standard method for ship manoeuvring predictions*. J Mar Sci Technol, vol. 20, pp. 37-52

Yoshimura, Y. (2005) *Mathematical Model for Manoeuvring Ship Motion (MMG Model)*. Workshop on Mathematical Models for Operations involving Ship-Ship Interaction, Tokyo, Japan, August

Yu, Ker-Wei and Wu, Chen-En, (2004) *Tracking control of a ship by PI-type sliding controller*, Journal of Marine Science and Technology, vol. 12, no. 3, pp. 183-188

Zlatev, Z., Milanov, E., Chotukova, V., Sakamoto, N., and Stern, F. (2009) *Combined Model-Scale EFD-CFD Investigation of the Maneuvering Characteristics of a High Speed Catamaran.* 10th International Conference on Fast Sea Transporation Fast, pp. 449-462, Greece

Zaojan, I.Z., (2006). *Ship Manoeuvring and Seakeeping*, Lecture Notes, Shanghai Jiao Tong University.

LIST OF PUBLICATIONS

Book Chapter

- **Pandey, J.** and Hasegawa, K. "Fuzzy Waypoint Guidance Controller for Wave Adaptive Modular Vessel (WAM-V)", a book chapter in Springer Book Series Studies in Computational Intelligence, 2017.**(Under Review)**
- **Pandey, J**. and Hasegawa, K. "Path Following of Underactuated Catamaran Surface Vessel (WAM-V) using FuzzyWaypoint Guidance Algorithm", pp. 995-1000, IEEE Intellisys, Sep 21-22, **London**, 2016. **Indexed in the series "Lecture Notes on Network and Systems", Springer Link Digital Library**

Peer Reviewed Conferences

- **Pandey, J.** and Hasegawa, K. "Autonomous Navigation of Catamaran Surface Vessel", IEEE OES Symposium on Underwater Technology (UT), pp. 1-6, **Busan**, 2017
- **Pandey, J.** and Hasegawa, K. "Study on Turning Manoeuvre of Catamaran Surface Vessel with a Combined Experimental and Simulation Method", vol. 49, pp. 446-451, 10^{th} IFAC Conference on Control Applications in Marine System CAMS, Sep 11-16, **Trondheim, Norway,** 2016
- **Pandey, J.** and Hasegawa, K. "Study on Manoeuverability and Control of an Autonomous Wave Adaptive Modular Vessel (WAM-V) for Ocean Observation", IEEE, International Association of Institutes of Navigation (IAIN) World Congress, pp. 1-7, **Prague, Chez Republic**, 2015

International and Domestic Conferences

- **Pandey, J.** and Hasegawa, K. "Manoeuvring Mathematical Model of Catamaran Wave Adaptive Modular Vessel (WAM-V) using the System Identification Technique", Proceedings of 7th PAAMES and AMEC2016 13-14 Oct., **Hong Kong**, 2016
- **Pandey, J.** and Hasegawa, K. "Study on Navigation and Control of the propelling Manoevre of Wave Adaptive Modular Vessel (WAM-V)", Asian Navigation Conference (ANC), **Kita Kyushu, Japan**, 2015
- **Pandey, J.** and Hasegawa, K. "Real Time Color Detection of a Light Buoy Aids to Navigation of an Autonomous Ship", Japan Society of Naval Architecture and Ocean Engineering (JASNAOE), **Nagasaki, Japan**, 2014